



# Families of regular spacetimes and energy conditions

Zi-Liang Wang  <sup>a</sup> Emmanuele Battista  <sup>b</sup>

<sup>a</sup>Department of Physics, School of Science, Jiangsu University of Science and Technology, Zhenjiang, 212003, China

<sup>b</sup>Istituto Nazionale di Fisica Nucleare, Laboratori Nazionali di Frascati, 00044 Frascati, Italy

E-mail: [ziliang.wang@just.edu.cn](mailto:ziliang.wang@just.edu.cn),  
[ebattista@lnf.infn.it](mailto:ebattista@lnf.infn.it), [emmanuelebattista@gmail.com](mailto:emmanuelebattista@gmail.com)

**Abstract.** We present a systematic method for constructing static, spherically symmetric regular spacetimes in general relativity satisfying the weak energy condition.

Our approach relies on physically reasonable assumptions on the matter energy density, together with the boundedness of the Kretschmann scalar. The latter property ensures the finiteness of all curvature invariants and, for the configurations considered, is equivalent to the completeness of causal geodesics. By classifying admissible density profiles according to their complexity, we recover well-known regular black hole solutions such as the Bardeen, Hayward, and Dymnikova models, which are thus naturally embedded in a unified and broader framework. Within this setting, we also derive closed-form expressions for several new families of regular geometries involving hypergeometric or incomplete Gamma functions, which in many cases reduce to elementary functions including algebraic, logarithmic, arctangent, and exponential forms. The emergence of horizons and photon spheres, as well as matching conditions to a Schwarzschild exterior, are also investigated.

**Keywords:** Regular spacetimes; Regular black holes; Classical energy conditions; Curvature invariants; Photon spheres; Junction conditions.

---

## Contents

<b>1</b>	<b>Introduction</b>	<b>1</b>
<b>2</b>	<b>General framework and regularity conditions</b>	<b>3</b>
2.1	Geometry and curvature invariants	4
2.2	The role of energy conditions	5
2.3	Sufficient conditions for regular spacetimes under the WEC	7
<b>3</b>	<b>Families of regular spacetimes from admissible density profiles</b>	<b>9</b>
3.1	Rational-falloff density profiles: $\rho(r) = \rho_0 [1 + (r/r_d)^n]^{-1}$	11
3.1.1	Logarithmically corrected geometries ( $n = 3$ )	12
3.1.2	Arctan-modified geometries ( $n = 6$ )	12
3.1.3	Mixed arctan and logarithmic geometries ( $n = 4$ )	13
3.2	Power-law density profiles: $\rho(r) = \rho_0 [1 + (r/r_d)^n]^{-\ell}$	14
3.2.1	Bardeen, Hayward, and other regular black holes ( $\ell = 1 + 3/n$ or $n = 3$ )	15
3.2.2	The case $n = 3/2$	16
3.2.3	Analytic patterns for solutions with even values of $n$	17
3.3	Exponentially suppressed density profiles: $\rho(r) = \rho_0 \exp[-(r/r_d)^n]$	19
3.3.1	Dymnikova black hole ( $n = 3$ )	19
3.3.2	New regular solutions ( $n = 3/2$ )	20
3.4	The composite density profiles $\rho(r) = \rho_0 (r/r_d)^\ell \exp[-(r/r_d)^n]$ and $\rho(r) = \rho_0 (r/r_d)^\kappa [1 + (r/r_d)^n]^{-\ell}$	20
3.5	Superposition of regular solutions	21
<b>4</b>	<b>Horizons and photon spheres</b>	<b>22</b>
<b>5</b>	<b>Junction conditions</b>	<b>25</b>
5.1	Impossibility of a smooth matching	25
5.2	Formation of a thin shell	26
<b>6</b>	<b>Concluding remarks</b>	<b>26</b>
<b>A</b>	<b>Riemann tensor components and Zakhary-McIntosh invariants</b>	<b>27</b>
<b>B</b>	<b>Kretschmann scalar for generic static, spherically symmetric spacetimes</b>	<b>31</b>
<b>C</b>	<b>Evaluation of the hypergeometric function <math>F(1, 3/4; 7/4; -r^4/r_d^4)</math></b>	<b>32</b>

---

## 1 Introduction

Soon after Einstein formulated the final version of his famous field equations, the first exact solution describing a static, spherically symmetric configuration was derived by Schwarzschild. This geometry exhibits two notable features: the presence of an event horizon and a central point,  $r = 0$ , where curvature becomes unboundedly large. Subsequent developments in our understanding of general relativity and its mathematical structure clarified that the former corresponds to a coordinate singularity that can be removed via a suitable choice of

coordinates, while the latter represents a true singularity, signaled by the incompleteness of causal geodesics. Similarly, homogeneous and isotropic cosmological scenarios, first devised by Friedmann shortly after Schwarzschild work, indicate a universe originated from a genuine singular state.

Singularities are generally regarded as signaling a breakdown of Einstein theory. For this reason, the initial reaction of several authors (see e.g. Ref. [1]) was to interpret them as artifacts of the high degree of symmetry underlying the known exact solutions of Einstein equations [2–4]. Nevertheless, this viewpoint had to be withdrawn with the advent of Hawking-Penrose theorems, which proved that singularities do arise as a generic consequence of the global causal structure of spacetime under physically reasonable assumptions [5–8]. These encompass the classical energy conditions, which encode standard constraints on matter, such as the positivity of the energy density and the requirements underlying the focusing of geodesics [9, 10].

Despite their foundational importance, classical energy criteria are known to be not fulfilled in various semiclassical and quantum contexts, most notably in the Casimir effect and Hawking radiation [9, 10], and even at the classical level, with traversable wormholes providing a prominent example [11, 12]. These circumstances have motivated a more refined investigation of the interplay between energy conditions and the global structure of spacetime.

One particularly active area where this relationship becomes manifest is the construction of regular, singularity-free geometries, which are widely explored in the literature, mostly as alternatives to the standard black hole paradigm [13–16]. Following Bardeen seminal proposal, based on an effective metric *ansatz* smoothly interpolating between an asymptotically Schwarzschild-like exterior and a de Sitter-like interior [17], notable de Sitter-core models were devised by Dymnikova [18], Hayward [19], and Frolov and Zelnikov [20], along with numerous subsequent extensions (a non-exhaustive list includes Refs. [21–33]). It was later realized [34, 35] that Bardeen metric can arise as an exact solution of Einstein gravity coupled to nonlinear electrodynamics, a framework that has since been extensively developed owing to its ability to embed regular configurations into a consistent field-theoretic setting [36–42]. Other approaches comprise those incorporating quantum corrections [43–46], those sourced by a variable equation-of-state fluid [47, 48], and those bearing a Minkowski core [49, 50], as well as interpolating black-bounce scenarios [51–53], models arising in extended theories of gravity [54–56], and others exhibiting metric signature changes [57, 58].

In many constructions, the regularization mechanism entails the violation of one or more classical energy criteria within a finite domain, consistently with the implications of singularity theorems (see e.g. Ref. [59]). However, the precise connection between regularity and energy conditions is subtle. Spacetime regularity imposes restrictions on the behavior of the metric and curvature invariants, which in turn translate into relations for the energy density and pressures through the Einstein equations. Whether these constraints are compatible with the energy criteria depends sensitively on the functional form of the matter distribution. Therefore, a systematic and model-independent analysis in this direction is desirable.

Motivated by these considerations, in this paper, we introduce a method for constructing families of static, spherically symmetric geometries of Kerr-Schild type that are regular and satisfy at least the weak energy condition. The primary input of our procedure is the matter energy density, which is subject to physically reasonable boundary and monotonicity assumptions. The ensuing solution of the Einstein field equations has finite curvature invariants, a feature that also guarantees, under the hypotheses employed in this work, the completeness of causal geodesics.

Within our approach, several well-known regular models can be understood as belonging to a broader and unified framework, in which they are recovered for particular choices of the parameters characterizing the energy-density profiles. In this general setting, enriched by the possibility of resorting to the superposition principle, new regular configurations can be naturally identified, and their compatibility with the energy conditions can be determined in a transparent manner. This allows us to establish a complete pattern connecting regularity, energy conditions, and the functional freedom underlying the construction of static, spherically symmetric metrics.

The plan of the paper is as follows. In Sec. 2, we introduce the geometric setup, discuss curvature invariants, and derive constraints ensuring regularity and compatibility with the weak energy condition. Then, in Sec. 3, we construct and classify several families of regular solutions generated by different classes of energy-density profiles, organized according to their complexity. Horizons and photon spheres associated with the resulting spacetimes are investigated in Sec. 4, while the matching procedure to an exterior vacuum region is addressed in Sec. 5. Finally, we draw our conclusions in Sec. 6. Supplementary material is given in the appendices.

*Conventions.* We use  $G = c = 1$  units, and metric signature  $(-+++)$ .

## 2 General framework and regularity conditions

In this paper, we consider static, spherically symmetric metrics of Kerr-Schild type [12, 60–62]

$$ds^2 = g_{\mu\nu} dx^\mu dx^\nu = -B(r) dt^2 + B^{-1}(r) dr^2 + r^2 d\Omega^2, \quad (2.1)$$

where  $d\Omega^2 = d\theta^2 + \sin^2\theta d\phi^2$  denotes the line element on the unit two-sphere.

Typically, two distinct methods can be pursued to assess whether a solution is regular [14, 54]. One relies on the finiteness of curvature scalars, while the other is a “coordinate-based” approach (in the sense that it involves, in practice, the choice of a coordinate system) rooted in the completeness of causal geodesics. The two paradigms are generally not tantamount, as there exist models complying with one notion while violating the other [4, 63, 64]. However, for the one-function setup (2.1), the two definitions were shown in Ref. [54] to be equivalent for strictly asymptotically flat geometries possessing regular cores. As we discuss below, this equivalence can be extended to a broader class of metrics displaying the (weaker) asymptotic Minkowskian behavior. Therefore, for the configurations considered in this work, we can safely characterize regularity by the absence of curvature singularities.

Curvature invariants of the metric (2.1) are examined in Sec. 2.1, where we also discuss assumptions that guarantee their boundedness at  $r = 0$ . Afterward, in Sec. 2.2, we consider classical energy conditions and show that the weak and strong ones cannot be valid simultaneously. For this reason, in Sec. 2.3, we focus on the null and weak energy criteria, and develop a general procedure for constructing regular spacetimes adhering to them.

## 2.1 Geometry and curvature invariants

In the geometry (2.1), the Ricci, Kretschmann, and Weyl scalars take the form, respectively,

$$R = g^{\mu\nu} R_{\mu\nu} = -B''(r) - \frac{2[2rB'(r) + B(r) - 1]}{r^2}, \quad (2.2a)$$

$$K := R_{\mu\nu\rho\sigma} R^{\mu\nu\rho\sigma} = B''(r)^2 + \frac{4B'(r)^2}{r^2} + \frac{4[B(r) - 1]^2}{r^4}, \quad (2.2b)$$

$$\mathcal{I}_1 := C_{\mu\nu\rho\sigma} C^{\mu\nu\rho\sigma} = \frac{[r^2 B''(r) - 2rB'(r) + 2B(r) - 2]^2}{3r^4}, \quad (2.2c)$$

where a prime denotes henceforth differentiation with respect to the radial variable  $r$ . In spherically symmetric spacetimes, some invariants involving the Hodge dual vanish identically, including the Chern-Pontryagin scalar  $K_2 := {}^*R_{\alpha\beta\mu\nu} R^{\alpha\beta\mu\nu}$  and the second Weyl invariant  $\mathcal{I}_2 := {}^*C_{\alpha\beta\mu\nu} C^{\alpha\beta\mu\nu}$  [65] (which turn out to be equivalent [66]). Other scalars can be expressed in terms of those listed above, such as the Ricci tensor squared and Euler invariant, which read, respectively [66–69],

$$R_{\mu\nu} R^{\mu\nu} = \frac{K - \mathcal{I}_1}{2} + \frac{R^2}{6}, \quad (2.3)$$

$$K_3 := {}^*R_{\alpha\beta\mu\nu} {}^*R^{\alpha\beta\mu\nu} = K - 2\mathcal{I}_1 - \frac{R^2}{3}. \quad (2.4)$$

Besides the standard polynomial curvature scalars, it is often useful to characterize the geometry through the full set of Zakhary-McIntosh invariants [14, 70–72], which consists of seventeen elements constructed from the Ricci and Weyl tensors in four-dimensional Lorentzian spaces. These quantities provide a systematic diagnostic of possible curvature singularities and of the algebraic structure of the gravitational field. Typically, the collection (2.2) constitutes a representative subset of these seventeen independent scalars [66, 68], and is generally sufficient to capture spacetime regularity [50].

However, as we demonstrate in Appendix A, the Riemann tensor components, as well as *all* curvature invariants, can be expressed as polynomials with constant coefficients in the three functions  $X(r)$ ,  $Y(r)$ , and  $Z(r)$  defined by

$$X(r) := \frac{B''(r)}{2}, \quad (2.5a)$$

$$Y(r) := \frac{B'(r)}{2r}, \quad (2.5b)$$

$$Z(r) := \frac{1 - B(r)}{r^2}. \quad (2.5c)$$

Remarkably, we find that the Kretschmann scalar (2.2b) constitutes a positive-definite quadratic form in  $X$ ,  $Y$ , and  $Z$ , as it is given by

$$K = 4(X^2 + 4Y^2 + Z^2). \quad (2.6)$$

Consequently, the finiteness of  $X$ ,  $Y$ , and  $Z$  implies the finiteness of  $K$ , and hence of all other algebraic curvature invariants, including the full Zakhary-McIntosh set. This proves that the Kretschmann scalar *alone* is sufficient to fully determine the curvature regularity of static, spherically symmetric metrics (2.1). Notably, this result also extends to two-function settings with  $g_{rr}g_{tt} \neq -1$ , as we show in detail in Appendix B.

Given the above premises, let us now focus on the conditions ensuring the absence of curvature singularities at  $r = 0$  (the asymptotic regime  $r \rightarrow \infty$  will be considered in Sec. 2.3). Assuming that the function  $B(r)$  admits a power-law expansion around  $r = 0$ ,

$$B(r) = B_0 + B_1 r + B_2 r^2 + B_3 r^3 + \mathcal{O}(r^4), \quad (2.7)$$

it follows immediately from identity (2.6) that

$$B_0 = 1, \quad B_1 = 0, \quad (2.8)$$

are necessary and sufficient for the Kretschmann scalar to remain bounded at  $r = 0$ . No restrictions on  $B_2$  and  $B_3$  arise at this stage, yet they will emerge once the energy conditions are taken into account.

## 2.2 The role of energy conditions

Classical energy conditions configure as pointwise inequalities involving the components of the stress-energy tensor that embody physically motivated assumptions on matter fields entering Einstein field equations. They are formulated as [9, 10]

$$T_{\mu\nu} k^\mu k^\nu \geq 0, \quad (2.9)$$

$$T_{\mu\nu} v^\mu v^\nu \geq 0, \quad (2.10)$$

$$\left( T_{\mu\nu} - \frac{1}{2} T g_{\mu\nu} \right) v^\mu v^\nu \geq 0, \quad (2.11)$$

$$T_{\mu\nu} v^\mu v^\nu \geq 0 \quad \text{and} \quad J^\mu J_\mu \leq 0, \quad (2.12)$$

where  $k^\mu$  is a null vector,  $v^\mu$  a normalized timelike vector,  $T = g^{\mu\nu} T_{\mu\nu}$  the trace of the stress-energy tensor, and  $J^\mu = -T^\mu{}_\nu v^\nu$  the energy flux vector. The first relation defines the null energy condition (NEC) and represents the minimal requirement for the focusing of null geodesics, while the second, referred to as weak energy condition (WEC), demands that the local energy density measured by any timelike observer be non-negative, thereby excluding the presence of exotic matter. The third inequality corresponds to the strong energy condition (SEC), which imposes that gravity is generically attractive, while the last one, the dominant energy condition (DEC), asserts that energy propagation is causal. Accordingly, the following implications hold:

$$\begin{aligned} \text{WEC} &\Rightarrow \text{NEC}, \\ \text{SEC} &\Rightarrow \text{NEC}, \\ \text{DEC} &\Rightarrow \text{NEC, WEC}. \end{aligned} \quad (2.13)$$

The standard approach to evaluating energy criteria is to introduce the local orthonormal basis carried by a static observer. This frame can be constructed via the tetrad field  $e^a{}_\mu$  [73, 74], which constitutes a  $4 \times 4$  matrix with positive determinant satisfying the completeness relation

$$g_{\mu\nu} = e^a{}_\mu e^b{}_\nu \eta_{ab}, \quad (2.14)$$

with its inverse  $e_a{}^\mu$  obeying the orthonormality condition

$$g_{\mu\nu} e_a{}^\mu e_b{}^\nu = \eta_{ab}. \quad (2.15)$$

Here,  $\eta_{ab} = \text{diag}(-1, 1, 1, 1)$  is the Minkowski metric, and Latin indices label frame components.

When projected onto the static frame, the energy-momentum tensor attains the diagonal form [4, 75]

$$T_{ab} = T_{\mu\nu} e_a^\mu e_b^\nu = \text{diag}(\rho, p_1, p_2, p_3), \quad (2.16)$$

where  $\rho$  denotes the total density of mass-energy,  $p_1$  the radial pressure,  $p_2$  and  $p_3$  the tangential pressures [11, 76], and

$$e_a^\mu = \begin{cases} \text{diag} [1/\sqrt{B}, \sqrt{B}, 1/r, 1/(r \sin \theta)], & (B > 0), \\ \text{diag} [1/\sqrt{-B}, \sqrt{-B}, 1/r, 1/(r \sin \theta)], & (B < 0), \end{cases} \quad (2.17)$$

which is a standard result for the geometry (2.1). In this way, the classical energy relations (2.9)–(2.12) read as [75]

$$\text{NEC} \Leftrightarrow \rho + p_i \geq 0, \quad (2.18a)$$

$$\text{WEC} \Leftrightarrow \rho \geq 0, \rho + p_i \geq 0, \quad (2.18b)$$

$$\text{SEC} \Leftrightarrow \rho + \sum_i p_i \geq 0, \rho + p_i \geq 0, \quad (2.18c)$$

$$\text{DEC} \Leftrightarrow \rho \geq 0, \rho \geq |p_i|, \quad (2.18d)$$

for all  $i = 1, 2, 3$ . We note that the diagonalization of the energy-momentum tensor may break down at a (Killing) horizon  $r = r_h$  (where  $B(r_h) = 0$ ), since  $e_a^\mu$  becomes singular. Nevertheless, the energy conditions at the horizon can be obtained as the limit  $r \rightarrow r_h$  of Eq. (2.18), which is defined for  $B \neq 0$  [77].

In the region where  $B(r) > 0$ , the Einstein field equations yield

$$\rho = \frac{1 - (rB)'}{8\pi r^2}, \quad (2.19a)$$

$$p_1 = \frac{(rB)' - 1}{8\pi r^2}, \quad (2.19b)$$

$$p_2 = p_3 = \frac{(rB)''}{16\pi r}, \quad (2.19c)$$

with the same formulas holding also in the domain  $B(r) < 0$ . This coincidence relies on the specific metric choice  $g_{rr}g_{tt} = -1$  underlying Eq. (2.1), since for more general static and spherically symmetric spacetimes with  $g_{rr}g_{tt} \neq \text{constant}$  (cf. Eq. (B.1)), the energy density and pressures generally take different forms depending on the sign of  $B(r)$ .

In the special isotropic-pressure scenario, corresponding to  $p_1 = p_2$  in Eq. (2.19), the function  $B(r)$  reduces to

$$B(r) = 1 - \frac{c_1}{r} + c_2 r^2, \quad (2.20)$$

and the energy criteria (2.18) imply

$$\rho = -\frac{3c_2}{8\pi}, \quad p_1 = p_2 = p_3 = -\rho, \quad (2.21)$$

with  $c_1$  and  $c_2$  arbitrary constants. Consequently, the NEC holds identically, while the WEC and DEC call simply for  $c_2 \leq 0$ . Enforcing regularity at  $r = 0$  further sets  $c_1 = 0$ , which results in a solution of either de Sitter type (for  $c_2 < 0$ ) or Minkowski type (for  $c_2 = 0$ ).

In the general configuration with anisotropic pressure, starting from the near-origin series (2.7), we find that the energy conditions lead to the constraints

$$B_0 = 1, \quad B_1 = 0, \quad B_2 = 0, \quad B_3 = 0. \quad (2.22)$$

In this case, one can show that the WEC and SEC cannot be simultaneously fulfilled for any nontrivial power-law expansion of  $B(r)$  near  $r = 0$ . The argument proceeds as follows. Suppose that the leading nonvanishing contribution to  $B(r)$  takes the form

$$B(r) = 1 + B_n r^n, \quad (2.23)$$

where we set  $n \geq 2$  in view of the regularity relations (2.8). Bearing in mind Eq. (2.19), the WEC entails  $\rho \geq 0$ , immediately yielding

$$B_n < 0, \quad (2.24)$$

while the SEC demands the tangential pressure  $p_2$  to be positive in a neighborhood of the origin, which amounts to

$$B_n > 0, \quad (2.25)$$

in clear contradiction with Eq. (2.24). Therefore, the WEC and SEC cannot be jointly satisfied, as anticipated before. This result is fully consistent with Hawking-Penrose theorems [5, 6], which indicate that avoiding singularities in regular spacetimes necessarily forces the violation of at least one of the classical energy conditions [9]<sup>1</sup>. For this reason, we hereafter restrict our attention to the NEC and WEC and search for families of regular spacetimes compatible with them.

### 2.3 Sufficient conditions for regular spacetimes under the WEC

To construct a regular spacetime satisfying the NEC and WEC, the following requirements must be fulfilled for any  $r \geq 0$ :

$$\rho(r) \geq 0 \text{ and finite}, \quad (2.26a)$$

$$\rho(r) + p_i(r) \geq 0 \text{ and finite}, \quad (2.26b)$$

$$K(r) \text{ remains finite}, \quad (2.26c)$$

the latter constraint reflecting the regularity analysis carried out in Sec. 2.1 (and Appendix A).

To broaden the scope of the analysis, we no longer assume the near-zone expansion (2.7). Instead, Eq. (2.19a) suggests introducing the mass function [4]

$$m(r) \equiv 4\pi \int_0^r \rho(\tilde{r}) \tilde{r}^2 d\tilde{r}, \quad (2.27)$$

which allows the metric component  $B(r)$  to be written, in full generality, as

$$B(r) = 1 - \frac{2m(r)}{r}. \quad (2.28)$$

---

<sup>1</sup>There exist alternative scenarios, such as defect spacetimes [78, 79], where curvature singularities may be avoided without violating the standard energy conditions. These constructions usually involve degenerate metrics and thus lie beyond the scope of classical general relativity (see also Refs. [80, 81] for cosmological applications). We do not consider such cases in this work.



Here,  $m(r)$  equals the Misner-Sharp-Hernandez mass, a key quantity for assessing the asymptotic flatness of spherically symmetric configurations defined as  $\mathcal{M} := \left(\frac{r}{2}\right) (1 - g^{\mu\nu} \nabla_\mu r \nabla_\nu r)$  [82]. Therefore, using identity (2.6) jointly with Einstein-equation relations (2.19), we find

$$\rho(r) + p_1(r) = 0, \quad (2.29)$$

$$\rho(r) + p_2(r) = -\frac{r}{2}\rho'(r) = \rho(r) + p_3(r), \quad (2.30)$$

$$K(r) = \frac{48 m(r)^2}{r^6} - \frac{64\pi m(r)}{r^3} [2\rho(r) - r\rho'(r)] + 64\pi^2 [4\rho(r)^2 + r^2\rho'(r)^2]. \quad (2.31)$$

It then follows from relations (2.26) that a set of *sufficient* conditions to construct a regular spacetime satisfying the WEC (and hence the NEC) is

$$\rho(r) \geq 0, \quad (2.32a)$$

$$\rho'(r) \leq 0, \quad (2.32b)$$

$$\rho(r) \in C^1. \quad (2.32c)$$

Regarding the remaining energy criteria, the DEC is not enforced at this stage, since it would introduce the additional inequality  $\rho + r\rho'/4 \geq 0$ , which cannot be straightforwardly incorporated within our framework; the SEC is likewise excluded, as we have already shown that it cannot hold simultaneously with the WEC.

Assumptions (2.32a) and (2.32b) are necessary and sufficient for the validity of the WEC, while Eq. (2.32c) is sufficient for the spacetime regularity at any finite radius, and entails that the functions (2.5), and consequently all curvature invariants, remain bounded for any finite  $r$ . In particular, since  $\rho(r)$  is supposed to be continuously differentiable, it admits the first-order expansion  $\rho(r) = \rho(0) + \rho'(0)r + o(r)$  as  $r \rightarrow 0^+$ . Substituting this into the definition (2.27) of  $m(r)$ , yields

$$m(r) = 4\pi \int_0^r [\rho(0) + \rho'(0)\tilde{r} + o(\tilde{r})] \tilde{r}^2 d\tilde{r} = \frac{4\pi}{3}\rho(0)r^3 + o(r^3). \quad (2.33)$$

Hence, by the definition of little- $o$ ,

$$\lim_{r \rightarrow 0} \frac{m(r)}{r^3} = \frac{4\pi}{3}\rho(0), \quad (2.34)$$

which is finite under our hypotheses. The quantity  $m(r)/r^3$  is thus regular at the center.

To restrict attention to physically reasonable scenarios, we further take into account the two additional assumptions

$$\rho'(0) = 0, \quad (2.35a)$$

$$\lim_{r \rightarrow \infty} B(r) = 1. \quad (2.35b)$$

The former accounts for a flat density profile at the core. This is a necessary condition for a static, locally isotropic matter distribution to maintain mechanical equilibrium at the origin and, in turn, naturally leads to a maximally symmetric geometry (locally de Sitter or Minkowski) [39], described near  $r = 0$  by Eq. (2.20) with  $c_1 = 0$ . Relation (2.35b) ensures that the metric approaches the Minkowski form asymptotically so that curvature scalars remain finite at spatial infinity. This means that, under our hypotheses, curvature invariants do not diverge anywhere in the spacetime.

As first shown in Ref. [54], regularity may be characterized through the absence of curvature singularities, as this notion is equivalent to geodesic completeness for Kerr-Schild geometries (2.1) possessing a regular core and strict asymptotic flatness (namely, configurations for which the Misner-Sharp-Hernandez mass  $m(r)$  approaches a finite nonvanishing value at infinity). We can now see that this result can be generalized, as Eq. (2.35b) is sufficient for the divergence argument underlying the completeness of null geodesics. Indeed, using Gullstrand-Painlevé coordinates  $(t_*, r, \theta, \phi)$ , one easily finds [54] that the time  $t_*$  associated with an ingoing radial light ray traveling from spatial infinity down to the center  $r = 0$  is

$$t_* = - \int_{\infty}^0 \frac{dr}{1 + \sqrt{2m(r)/r}}. \quad (2.36)$$

The quantity  $t_*$  blows up to  $-\infty$  whenever  $m(r)/r \rightarrow 0$  as  $r \rightarrow \infty$ , or equivalently when Eq. (2.35b) holds. Indeed, in this limit the term  $\sqrt{2m(r)/r}$  becomes negligible, so that the integrand approaches unity at large  $r$  and the integral diverges linearly. In addition, completeness of timelike geodesics stems from core regularity (2.34), as proved in Ref. [54]. Therefore, the equivalence between causal geodesic completeness and the finiteness of curvature scalars extends beyond the strictly asymptotically flat scenario and remains valid also for metrics approaching the Minkowski form at infinity. This applies, in particular, to all regular solutions considered in this paper.

We can thus conclude that the system of ordinary differential equations (2.29)–(2.31) provides a systematic algorithm for deriving families of regular solutions adhering to the WEC: once a density profile  $\rho(r)$  obeying Eq. (2.32) is given, the corresponding metric component  $B(r)$  follows directly from solving Eq. (2.19a). Explicit applications of this scheme will be the main focus of the next section.

### 3 Families of regular spacetimes from admissible density profiles

In this section, we employ the algorithm introduced before and explore various regular spacetimes adhering to WEC and sourced by a mass-energy density  $\rho(r)$  complying with relations (2.32) and (2.35a). The different cases analyzed admit the general parametrization

$$\rho(r) = \rho_0 F(r), \quad (3.1)$$

where  $\rho_0 \equiv \rho(0)$  denotes the central density and  $F(r)$  is a dimensionless shape function containing a characteristic length scale  $r_d$ , normalized so that  $F(0) = 1$ . We therefore set aside regular scenarios with  $F(0) = 0$  (which have also been proposed in the literature [49, 50]), since they lead to Minkowski-core configurations where typically  $\rho'(r) > 0$  over some interval of  $r$ , thereby violating the NEC (cf. Eq. (2.32b)).

To organize the admissible profiles in a systematic way, we introduce a parameter  $\mathcal{C}$  that quantifies the functional complexity of  $\rho(r)$ . This quantity is not intended to establish a unique or universal definition of complexity, but rather provides a practical tool for classifying the parametric forms of  $\rho(r)$  according to their structural simplicity. In this way, we can study regular geometries starting from minimally complex densities and gradually proceeding to more elaborate cases.

We define the factor  $\mathcal{C}$  as

$$\mathcal{C} := N_{\text{param}} + N_{\text{op}} + \alpha N_{\text{comp}}, \quad (3.2)$$

where

- $N_{\text{param}}$  denotes the number of free, dimensionless *shape parameters* that affect the functional form of  $\rho(r)$ , excluding the overall normalization  $\rho_0$  and the length scale  $r_d$ ;
- $N_{\text{op}}$  counts the number of elementary operations required to construct  $\rho(r)$ , including addition, subtraction, multiplication, division, and algebraic power operations;
- $N_{\text{comp}}$  tallies the number of *nontrivial* elementary function compositions, such as  $\exp(f)$  or  $\ln(1 + f)$ , where  $f = f(r)$ ;
- $\alpha$  is a weighting factor controlling the relative importance of compositions, and we set  $\alpha = 2$  for simplicity.

Category	Function $F(x)$	$N_{\text{param}}$	$N_{\text{op}}$	$N_{\text{comp}}$	$\mathcal{C}$
Examples of basic functions	$1/x$	0	0	0	0
	$1/x^2$	0	1	0	1
	$(1 + x^2)^{-1}$	0	2	0	2
	$\exp(-x)$	0	0	1	2
Shape functions studied in this paper	$(1 + x^n)^{-1}$	1	2	0	3
	$\exp(-x^n)$	1	1	1	4
	$(1 + x^n)^{-\ell}$	2	3	0	5
	$x^\ell \exp(-x^n)$	2	3	1	7
	$x^\kappa (1 + x^n)^{-\ell}$	3	5	0	8

**Table 1:** Shape functions  $F(x)$  (with  $x := r/r_d$ ) and their associated functional complexity  $\mathcal{C}$ . Since  $\mathcal{C}$  is designed to capture the structural hierarchy of functional forms, algebraically equivalent expressions, including sign changes and reciprocal representations, are assigned the same complexity factor. Accordingly, we set  $N_{\text{op}} = 0$  for  $F(x) = 1/x$ , so that  $F(x) = x^n$  and  $F(x) = x^{-n}$  carry the same value of  $N_{\text{op}}$ , and the operation count does not depend on the sign of the shape parameter  $n$ .

Representative examples of functions, along with their corresponding complexity parameter, are listed in Table 1, which illustrates how increasingly elaborate functional structures naturally correspond to larger values of  $\mathcal{C}$ . As an example, the function  $F(x) = (1 + x^n)^{-1}$  (with  $x := r/r_d$ ) has  $\mathcal{C} = 3$ : it contains the dimensionless exponent  $n$  ( $N_{\text{param}} = 1$ ), involves two elementary operations (one addition and one power, so  $N_{\text{op}} = 2$ ), and includes no trivial compositions ( $N_{\text{comp}} = 0$ ). Likewise,  $F(x) = x^\ell \exp(-x^n)$  has  $\mathcal{C} = 7$ : two shape parameters  $\ell$  and  $n$  ( $N_{\text{param}} = 2$ ), three elementary operations (two power operations and one multiplication and hence  $N_{\text{op}} = 3$ ), and one composition (the exponential function, which yields  $N_{\text{comp}} = 1$ ). Of course, many other possibilities exist beyond those listed in Table 1. For instance, regular black holes studied in Ref. [34] adopt hyperbolic density functions that spoil the NEC at the origin, and will therefore not be discussed here. However, in such a setup, the typical functions encountered are of the form  $F(r) \sim r^{-n} \text{sech}^2(r_d/r)$ , for which one typically finds  $\mathcal{C} > 10$ . These profiles are therefore to be regarded as highly complex, when expressed in terms of elementary functions.

Guided by the admissibility criteria (2.32) and (2.35a), we now investigate energy-density profiles in order of increasing values of  $\mathcal{C}$ , together with the ensuing geometries. We begin with the simplest rational-falloff forms (Sec. 3.1), then consider power-law functions (Sec. 3.2),

exponentially suppressed densities (Sec. 3.3), and finally composite constructions combining algebraic and exponential structures (Sec. 3.4). We conclude the section by discussing the possibility of superposing the resulting solutions (Sec. 3.5). For all examined configurations, compatibility with the WEC (or even the DEC) can be easily determined by inspecting the allowed ranges of the free parameters of the model.

### 3.1 Rational-falloff density profiles: $\rho(r) = \rho_0 [1 + (r/r_d)^n]^{-1}$

According to our definition (3.2) of functional complexity, the simplest form assumed by  $\rho(r)$  corresponds to the rational power-law falloff

$$\rho(r) = \frac{\rho_0}{1 + (r/r_d)^n}. \quad (3.3)$$

The relations (2.32), and consequently the WEC, are obeyed whenever  $n \geq 1$ . First, given the non-negativity assumption (2.32a), we take the  $r = 0$  density  $\rho_0$  to be positive (and finite). For  $n > 0$ , the monotonicity constraint (2.32b) is then automatically fulfilled, while the smoothness criterion (2.32c) calls for  $n \geq 1$ . This bound becomes more stringent once the central isotropy condition (2.35a) is imposed, which entails  $n > 1$ . Enforcing the DEC the additional inequality  $n \leq 4$  arises, which will be relaxed in the following to keep the discussion as general as possible.

The asymptotic flatness of the spacetime can be examined through the large- $r$  behavior of  $\rho(r)$ , which scales as  $\rho(r) \sim \rho_0 (r_d/r)^n$  for  $r \gg r_d$ . Substituting this into the formula (2.27) for the total enclosed mass yields

$$m(r) \sim \rho_0 (r_d)^n \int r^{2-n} dr, \quad (3.4)$$

and, accordingly, four distinct regimes can be identified, depending on the value of  $n$ :

- $n > 3$ :  $m(r)$  converges as  $r \rightarrow \infty$ . This situation points to a finite ADM mass and a strictly asymptotically flat geometry.
- $n = 3$ : the mass function grows logarithmically, and hence the ADM mass fails to converge to a finite value at infinity. We thus find what we may call a “marginally asymptotically flat spacetime”, meaning that the metric approaches the Minkowski form at large  $r$  (i.e., it complies with Eq. (2.35b)), but with a falloff slower than  $1/r$ . As we will see in Sec. 3.1.1, such behavior generically leads to geometries involving logarithmic corrections (see also Refs. [83, 84]).
- $2 < n < 3$ :  $m(r)$  diverges as a power law, but more slowly than the linear function  $r$ . This again corresponds to a marginally asymptotically flat scenario.
- $n \leq 2$ :  $m(r)$  blows up with a growth rate equal to or faster than  $r$ , indicating a non-asymptotically flat solution. Such cases will not be considered in the present work.

With the *ansatz* (3.3), the metric function  $B(r)$ , obtained by solving Eq. (2.19a), can be formulated in terms of the Gauss hypergeometric function  $F(a, b; c; z) \equiv {}_2F_1(a, b; c; z)$  [85]. Explicitly, we find

$$B(r) = 1 + \frac{c_1}{r} - \frac{r^2 \lambda}{3r_d^2} F\left[1, \frac{3}{n}; 1 + \frac{3}{n}; -\left(\frac{r}{r_d}\right)^n\right], \quad (3.5)$$

with  $c_1$  an integration constant and  $\lambda := 8\pi\rho_0 r_d^2$  a dimensionless quantity. One can show that the Minkowski limit (2.35b) is achieved for  $n > 2$ , in agreement with our previous analysis. In this regime, spacetime regularity can equivalently be accommodated either by the boundedness of the Kretschmann scalar (2.6) or by the completeness of causal geodesics.

From the above result, we also see that the only freedom in the algorithm devised in Sec. 2.3 for constructing regular WEC-respecting solutions concerns the constant  $c_1$ . Whether  $c_1$  vanishes or not depends on the behavior of  $B(r)$  near the origin (for instance, we will see that it is zero for the logarithmic solution (3.9), while remaining nonzero for the black hole geometry (3.43)).

For specific values of the parameter  $n$ , the hypergeometric function admits a representation in terms of elementary contributions. The special cases  $n = 3$  and  $n = 6$  are analyzed in Secs. 3.1.1 and 3.1.2, respectively; to illustrate a representative generic scenario, the configuration with  $n = 4$  is studied in Sec. 3.1.3.

### 3.1.1 Logarithmically corrected geometries ( $n = 3$ )

In the situation with  $n = 3$ , the hypergeometric function entering Eq. (3.5) takes the closed-form expression [85]

$$F(1, 1; 2; z) = -\frac{\ln(1-z)}{z}, \quad (3.6)$$

which allows us to write

$$B(r) = 1 + \frac{c_1}{r} - \frac{\lambda r_d}{3r} \ln\left(\frac{r^3}{r_d^3} + 1\right). \quad (3.7)$$

The small- $r$  expansion

$$B(r) = 1 + \frac{c_1}{r} - \frac{\lambda}{3r_d^2} r^2 + \mathcal{O}(r^2), \quad (3.8)$$

shows that regularity at the origin enforces  $c_1 = 0$ , thereby leading to a spacetime with a central de Sitter core. Therefore, we end up with the regular and marginally asymptotically flat solution

$$B(r) = 1 - \frac{\lambda r_d}{3r} \ln\left(\frac{r^3}{r_d^3} + 1\right). \quad (3.9)$$

As far as we are aware, this has not been reported previously in the literature and represents the lowest-complexity example of a logarithm-based regular geometry complying with WEC.

### 3.1.2 Arctan-modified geometries ( $n = 6$ )

For  $n = 6$ , we can exploit the identity [85]

$$F(1, 1/2; 3/2; -z^2) = \frac{\arctan z}{z}, \quad (3.10)$$

to recast Eq. (3.5) as

$$B(r) = 1 - \frac{\lambda r_d}{3r} \arctan\left(\frac{r^3}{r_d^3}\right), \quad (3.11)$$

where like before we have set  $c_1 = 0$ . In the asymptotic region  $r \gg r_d$ , we thus find

$$B(r) \sim 1 - \frac{2m_{\text{eff}}}{r}, \quad (3.12)$$

where  $m_{\text{eff}}$  denotes the effective ADM mass, here given by

$$m_{\text{eff}} = \frac{\pi \lambda r_d}{12}. \quad (3.13)$$

Therefore, Eq. (3.11) provides, to the best of our knowledge, the simplest realization of an arctan-based regular, strictly asymptotically flat spacetime obeying the WEC. Similar models arising from a phantom scalar field were previously presented in Ref. [86], but are formulated in a more involved metric representation.

### 3.1.3 Mixed arctan and logarithmic geometries ( $n = 4$ )

Leaving aside the special cases  $n = 3$  and  $n = 6$ , when  $n \geq 2$  the hypergeometric function occurring in Eq. (3.5) does not admit a compact closed form in terms of a single elementary function, but can still be reduced to a finite combination of elementary contributions, typically involving logarithmic and inverse-trigonometric terms. In this situation, the basic strategy for evaluating  $F(1, 3/n; 1 + 3/n; -z)$  is to start from its integral representation [85],

$$F(1, b; 1 + b; -z) = b \int_0^1 \frac{t^{b-1}}{1 + tz} dt, \quad (b \equiv 3/n), \quad (3.14)$$

and then exploit a partial-fraction decomposition.

As an explicit example, let us consider the parameter choice  $b = 3/4$ , which corresponds to fixing  $n = 4$ . By setting  $z \equiv (r/r_d)^4$  and performing the change of variables  $u = t^{1/4} r/r_d$ , Eq. (3.14) becomes

$$F[1, 3/4; 7/4; -(r/r_d)^4] = \frac{3r_d^3}{r^3} I(r), \quad (3.15a)$$

where we have introduced

$$I(r) := \int_0^{r/r_d} \frac{u^2}{1 + u^4} du. \quad (3.15b)$$

As detailed in Appendix C, one can prove that

$$I(r) = \frac{1}{2\sqrt{2}} \left\{ \arctan[\sqrt{2}(r/r_d) + 1] + \arctan[\sqrt{2}(r/r_d) - 1] \right\} + \frac{1}{4\sqrt{2}} \ln \left[ \frac{(r/r_d)^2 - \sqrt{2}(r/r_d) + 1}{(r/r_d)^2 + \sqrt{2}(r/r_d) + 1} \right]. \quad (3.16)$$

Therefore, upon exploiting Eq. (3.5) with  $c_1 = 0$ , we obtain the novel regular solution

$$B(r) = 1 - \frac{\lambda r_d}{r} I(r), \quad (3.17)$$

which gives rise to a strictly asymptotically flat spacetime featuring an effective ADM mass  $m_{\text{eff}} = \pi \lambda r_d / (4\sqrt{2})$  and a de Sitter core. These properties can be readily inferred from the asymptotic behavior of  $I(r)$ , namely

$$I(r) \xrightarrow{r \gg r_d} \frac{\pi}{2\sqrt{2}} - \frac{r_d}{r} + \mathcal{O}(r_d^2/r^2), \quad (3.18a)$$

$$I(r) \xrightarrow{r \ll r_d} \frac{r^3}{3r_d^3} + \mathcal{O}(r^5/r_d^5). \quad (3.18b)$$

For other values of  $n$ , the resulting geometries can also be regular, but they generally come with more complicated combinations of logarithmic and inverse-trigonometric functions. We shall not pursue these configurations further in this paper.

### 3.2 Power-law density profiles: $\rho(r) = \rho_0 [1 + (r/r_d)^n]^{-\ell}$

In this section, we deal with a mass-energy density with power-law falloff

$$\rho(r) = \frac{\rho_0}{[1 + (r/r_d)^n]^\ell}, \quad (3.19)$$

which represents an increase in functional complexity relative to the *ansatz* (3.3) (in this case  $\mathcal{C} = 5$ , see Table 1). Owing to Eq. (2.32a), we take  $\rho_0 > 0$  (and finite), while the requirement of monotonic decrease (2.32b) furnishes  $n\ell > 0$  (excluding the trivial setup of a constant density), as is clear from

$$\rho'(r) = -(n\ell \rho_0/r_d) (r/r_d)^{n-1} [1 + (r/r_d)^n]^{-\ell-1}. \quad (3.20)$$

The profile is continuous at  $r = 0$  for any positive  $n$ , and belongs to the class  $C^1$ , as mandated by Eq. (2.32c), provided  $n \geq 1$ . Thus, consistently with the sufficient criteria (2.32), the WEC is satisfied whenever  $n \geq 1$  and  $\ell > 0$ . If, in addition, the flat-core condition (2.35a) is imposed, the parameter space is further limited to

$$n > 1, \quad (3.21a)$$

$$\ell > 0. \quad (3.21b)$$

The DEC entails the tighter bound  $n\ell \leq 4$ , which however we do not enforce to retain generality in our analysis.

The asymptotic behavior of the Misner-Sharp-Hernandez mass (cf. Eq. (2.27))

$$m(r) \sim \rho_0 (r_d)^{n\ell} \int r^{2-n\ell} dr, \quad (3.22)$$

permits to distinguish the following scenarios:

- $n\ell > 3$ : the spacetime is strictly asymptotically flat, since the total mass converges at large distances.
- $n\ell = 3$ :  $m(r) \sim \ln r$ , yielding a marginally asymptotically flat solution. An explicit example is provided by  $n = 2$  and  $\ell = 3/2$ , which has been thoroughly examined in Ref. [87] (see Eq. (3.2) therein).
- $2 < n\ell < 3$ : the mass function  $m(r)$  blows up as a power law slower than  $r$ , resulting again in a marginally asymptotically flat solution.
- $n\ell \leq 2$ : the enclosed mass exhibits a power-law divergence of order comparable to or higher than  $r$ , signaling a non-asymptotically flat spacetime.

It is easy to see that the density profile (3.19) leads to the metric

$$B(r) = 1 + \frac{c_1}{r} - \frac{\lambda r^2}{3r_d^2} F\left[\ell, \frac{3}{n}; 1 + \frac{3}{n}; -\left(\frac{r}{r_d}\right)^n\right], \quad (3.23)$$

which exhibits the Minkowski asymptotics (2.35b) for  $n\ell > 2$ , consistently with the above discussion.

Below we focus on particular choices of the parameters  $n$  and  $\ell$  for which the hypergeometric function boils down to elementary contributions. Explicitly, we explore the two cases  $\ell = 1 + 3/n$ ,  $n = 3$  in Sec. 3.2.1, and  $n = 3/2$  in Sec. 3.2.2. Finally, in Sec. 3.2.3, we examine solutions with even values of  $n$  and present the analytic structure of the corresponding geometries for  $n = 2, 4, 6$ .

### 3.2.1 Bardeen, Hayward, and other regular black holes ( $\ell = 1 + 3/n$ or $n = 3$ )

The first interesting setup arises for  $\ell = 1 + 3/n$ , whence we find that Eq. (3.23) boils down to

$$B(r) = 1 + \frac{c_1}{r} - \frac{\lambda r^2}{3r_d^2} \left[ 1 + \left( \frac{r}{r_d} \right)^n \right]^{-3/n}, \quad (3.24)$$

by virtue of the identity  $F(a, b; a; z) = (1 - z)^{-b}$  [85].

Starting from the small-distance expansion of  $B(r)$ , it is easy to see that regularity requires a de Sitter core, which corresponds to setting  $c_1 = 0$  in Eq. (3.24). The resulting configuration embodies a class of strictly asymptotically flat geometries with effective ADM mass

$$m_{\text{eff}} = \frac{\lambda r_d}{6}, \quad (3.25)$$

provided the lower bound  $n > 1$  is taken into account, which guarantees that  $n\ell > 3$ .

Therefore, we end up with the function

$$B(r) = 1 - \frac{\lambda r^2}{3r_d^2} \left[ 1 + \left( \frac{r}{r_d} \right)^n \right]^{-3/n}, \quad (3.26)$$

which allows us to recover a family of regular black hole solutions well known in the literature [39, 87, 88]. In particular, our expression coincides with Eq. (3.20) of Ref. [87] upon setting  $\mu = 3$  therein.<sup>2</sup> Moreover, the cases  $n = 2$  and  $n = 3$  reproduce the functional forms of the Bardeen [17] and Hayward [19] regular black holes, respectively, after appropriate identifications of the parameters.

Let us now consider the scenario with  $n = 3$  and  $\ell > 1$ , which, in view of our analysis, produces a strictly asymptotically flat configuration. In this situation, starting from the general integral representation of the hypergeometric function (see Eq. (C.1)), we obtain

$$F(\ell, 1; 2; -z) = \int_0^1 \frac{dt}{(1 + zt)^\ell} = \frac{1 - (1 + z)^{1-\ell}}{(\ell - 1)z}, \quad (3.27)$$

and hence from Eq. (3.23) we arrive at

$$B(r) = 1 + \frac{1}{r} \left( c_1 - \frac{\lambda r_d}{3(\ell - 1)} \right) + \frac{\lambda r_d}{3(\ell - 1)r} \left( 1 + \frac{r^3}{r_d^3} \right)^{-\ell+1}. \quad (3.28)$$

In the limit  $r \rightarrow 0$ , one finds

$$B(r) = 1 + \frac{c_1}{r} - \frac{\lambda}{3r_d^2} r^2 + \mathcal{O}(r^5), \quad (3.29)$$

and hence regularity at the origin requires  $c_1 = 0$ . In this way, the large- $r$  expansion of  $B(r)$  becomes

$$B(r) = 1 - \frac{\lambda r_d}{3(\ell - 1)r} + \frac{\lambda r_d^{3\ell-2}}{3(\ell - 1)} r^{2-3\ell} + \mathcal{O}(r^{-3\ell-1}), \quad (3.30)$$

---

<sup>2</sup>This correspondence does not imply that our construction is less general than that of Ref. [87]. Here, we restrict attention to regular spacetimes satisfying the WEC, whereas Eq. (3.20) of Ref. [87] does not in general fulfill this requirement.



and we see that the matter-induced correction decays faster than  $1/r$  for  $\ell > 1$ , so that the effective ADM mass reads as

$$m_{\text{eff}} = \frac{\lambda r_d}{6(\ell - 1)}. \quad (3.31)$$

Hence, we obtain the family of regular spacetimes

$$B(r) = 1 - \frac{\lambda r_d}{3(\ell - 1)r} + \frac{\lambda r_d}{3(\ell - 1)r} \left(1 + \frac{r^3}{r_d^3}\right)^{-\ell+1}, \quad (3.32)$$

which has already appeared in the literature. For instance, as shown in Ref. [89], this metric can describe a black hole sourced by a specific dark-matter halo model for suitable choices of the free parameters (see Eq. (28) therein). In addition, consistently with the previous solution, the case  $\ell = 2$  again coincides with the Hayward black hole [19].

It should be noted that one may also take  $2/3 < \ell < 1$  in Eq. (3.32). However, in this range, the spacetime is only marginally asymptotically flat.

### 3.2.2 The case $n = 3/2$

When  $n = 3/2$ , it follows from Eq. (3.23) jointly with the integral representation of the underlying hypergeometric function (see Eq. (C.1)) that

$$B(r) = 1 + \frac{1}{r} \left( c_1 - \frac{2\lambda r_d}{3(\ell - 2)(\ell - 1)} \right) + \frac{2\lambda}{3(\ell - 2)(\ell - 1)} \frac{(\ell - 1)r^3 + \ell (r_d r)^{3/2} + r_d^3}{r_d^2 r} \left[ 1 + \left( \frac{r}{r_d} \right)^{3/2} \right]^{-\ell}, \quad (3.33)$$

where we assume  $\ell > 2$  owing to the asymptotic flatness condition.

The expansions for  $r \rightarrow 0$  and  $r \rightarrow \infty$  are, respectively,

$$B(r) = 1 + \frac{c_1}{r} - \frac{\lambda}{3r_d^2} r^2 + \mathcal{O}(r^{7/2}), \quad (3.34)$$

$$B(r) = 1 + \frac{1}{r} \left( c_1 - \frac{2\lambda r_d}{3(\ell - 2)(\ell - 1)} \right) + \frac{2\lambda r_d^{3\ell/2-2}}{3(\ell - 2)} r^{2-\frac{3\ell}{2}} + \mathcal{O}(r^{-\frac{3\ell}{2}-1}). \quad (3.35)$$

Therefore, the metric displays a nonsingular de Sitter core provided  $c_1 = 0$ , while, for  $\ell > 2$ , the third term on the right-hand side of Eq. (3.35) decays faster than  $1/r$ , yielding the effective ADM mass

$$m_{\text{eff}} = \frac{\lambda r_d}{3(\ell - 2)(\ell - 1)}. \quad (3.36)$$

In view of the above results, we derive the class of regular geometries

$$B(r) = 1 - \frac{2\lambda r_d}{3(\ell - 2)(\ell - 1)r} \left\{ 1 - \left[ (\ell - 1) \left( \frac{r}{r_d} \right)^3 + \ell \left( \frac{r}{r_d} \right)^{3/2} + 1 \right] \left[ 1 + \left( \frac{r}{r_d} \right)^{3/2} \right]^{-\ell} \right\}, \quad (3.37)$$

which, to the best of our knowledge, are presented here for the first time in the literature.

It is worth noticing that, upon relaxing the constraint  $\ell > 2$ , one can arrive at marginally asymptotically flat configurations. For instance, Eq. (3.37) with  $4/3 < \ell < 2$  gives a metric function that still approaches the Minkowski limit at large  $r$ , but with a power-law falloff slower than  $1/r$ . The borderline case  $\ell = 2$  yields

$$B(r) = 1 + \frac{2\lambda r_d}{3r} \left\{ \frac{(r/r_d)^{3/2}}{1 + (r/r_d)^{3/2}} - \ln \left[ 1 + (r/r_d)^{3/2} \right] \right\}, \quad (3.38)$$

which presents a characteristic logarithmic term.

### 3.2.3 Analytic patterns for solutions with even values of $n$

The models analyzed in the previous sections indicate that the general analytic structure of the metric component  $B(r)$  depends sensitively on the particular choice of the coefficients  $n$  and  $\ell$ , a feature that can be traced back to the underlying hypergeometric functions appearing in the general formula (3.23). Apart from the specific parameter combinations examined before (i.e.,  $\ell = 1 + 3/n$ ,  $n = 3$ , and  $n = 3/2$ ), we find that, remarkably, regular, strictly asymptotically flat geometries can be organized according to a systematic pattern for certain even values of  $n$ , depending on whether  $\ell$  is an integer or a half-integer.

For example, when  $n = 2$  and  $\ell$  is an integer larger than one (i.e.,  $\ell = 2, 3, 4, 5, \dots$ ),  $B(r)$  can be generically decomposed into the sum of a rational function  $\mathcal{R}_\ell(r^2)$  of  $r^2$  and a term proportional to  $r^{-1} \arctan(r/r_d)$ . Schematically, we can write

$$B(r) = 1 + \mathcal{R}_\ell(r^2) + \frac{c_\ell}{r} \arctan\left(\frac{r}{r_d}\right), \quad (3.39)$$

where  $c_\ell$  is a constant depending on  $\ell$ . In contrast, when  $\ell$  is a half-integer of the form  $\ell = (2k + 1)/2$  with  $k \in \mathbb{N}$ , the arctan contribution disappears and the solution reduces to a purely algebraic (fractional) expression involving powers of  $r^2$ . The special scenario with  $\ell = 3/2$  corresponds to a marginally asymptotically flat spacetime (since in this case  $n\ell = 3$ ), and thus contains a logarithmic factor.

An analogous structure emerges for  $n = 6$ . Indeed, an integer  $\ell$  gives rise to a decomposition into a rational function of  $r^2$  plus a term proportional to  $r^{-1} \arctan(r^3/r_d^3)$ , whereas a half-integer  $\ell = (2k + 1)/2$  leads to fractional forms comprising powers of  $r^2$  and no inverse trigonometric functions.

When  $n = 4$  and  $\ell$  is an integer, the metric typically consists of a fractional expression supplemented by the auxiliary function  $I(r)$  defined in Eq. (3.16), which includes both arctangent and logarithmic terms; by contrast, for half-integer  $\ell$ ,  $B(r)$  cannot be written in terms of elementary functions.

The analytic structures identified above are illustrated in Table 2, where we list sample regular solutions according to the values of  $n$  and  $\ell$ .

$n$	$\ell$	Metric function $B(r)$
2	$\frac{3}{2}$	$1 + \frac{\lambda r_d}{\sqrt{r^2 + r_d^2}} - \frac{\lambda r_d}{r} \ln \left( \frac{r + \sqrt{r^2 + r_d^2}}{r_d} \right)$
2	2	$1 + \frac{\lambda r_d}{2} \left[ \frac{r_d}{r^2 + r_d^2} - \frac{1}{r} \arctan \left( \frac{r}{r_d} \right) \right]$
2	3	$1 - \frac{\lambda r_d^2 (r^2 - r_d^2)}{8(r^2 + r_d^2)^2} - \frac{\lambda r_d}{8r} \arctan \left( \frac{r}{r_d} \right)$
2	$\frac{7}{2}$	$1 - \frac{\lambda r_d r^2 (5r_d^2 + 2r^2)}{15(r^2 + r_d^2)^{5/2}}$
2	4	$1 - \frac{\lambda r_d^2 (3r^2 - r_d^2) (r^2 + 3r_d^2)}{48 (r^2 + r_d^2)^3} - \frac{\lambda r_d}{16r} \arctan \left( \frac{r}{r_d} \right)$
2	$\frac{9}{2}$	$1 - \frac{\lambda r_d r^2 (8r^4 + 28r^2 r_d^2 + 35r_d^4)}{105 (r^2 + r_d^2)^{7/2}}$
2	5	$1 - \frac{\lambda r_d^2 (15r^6 + 55r^4 r_d^2 + 73r^2 r_d^4 - 15r_d^6)}{384 (r^2 + r_d^2)^4} - \frac{5\lambda r_d}{128r} \arctan \left( \frac{r}{r_d} \right)$
4	2	$1 - \frac{\lambda r_d^2 r^2}{4(r^4 + r_d^4)} - \frac{\lambda r_d}{4r} I(r)$
4	3	$1 - \frac{\lambda r_d^2 r^2 (5r^4 + 9r_d^4)}{32(r^4 + r_d^4)^2} - \frac{5\lambda r_d}{32r} I(r)$
6	1/2	$1 - \frac{\lambda r_d}{3r} \ln \left( \frac{r^3}{r_d^3} + \sqrt{1 + \frac{r^6}{r_d^6}} \right)$
6	2	$1 - \frac{\lambda r_d^4 r^2}{6(r^6 + r_d^6)} - \frac{\lambda r_d}{6r} \arctan \left( \frac{r^3}{r_d^3} \right)$
6	$\frac{5}{2}$	$1 - \frac{\lambda r_d r^2 (2r^6 + 3r_d^6)}{9 (r^6 + r_d^6)^{3/2}}$
6	3	$1 - \frac{\lambda r_d^4 r^2 (3r^6 + 5r_d^6)}{24 (r^6 + r_d^6)^2} - \frac{\lambda r_d}{8r} \arctan \left( \frac{r^3}{r_d^3} \right)$
6	$\frac{7}{2}$	$1 - \frac{\lambda r_d r^2 (8r^{12} + 20r^6 r_d^6 + 15r_d^{12})}{45 (r^6 + r_d^6)^{5/2}}$
6	4	$1 - \frac{\lambda r_d^4 r^2 (15r^{12} + 40r^6 r_d^6 + 33r_d^{12})}{144 (r^6 + r_d^6)^3} - \frac{5\lambda r_d}{48r} \arctan \left( \frac{r^3}{r_d^3} \right)$

**Table 2:** Representative regular metrics sourced by the generalized power-law density profile (3.19) for  $n = 2, 4, 6$  and integer or half-integer values of  $\ell$ . The solutions display a systematic analytic pattern. Geometries with  $n = 2$  and  $n = 6$  share a similar form, while those with  $n = 4$  involve the function  $I(r)$  (see Eq. (3.16)) when  $\ell$  is an integer. Furthermore, configurations satisfying  $n\ell = 3$  correspond to marginally asymptotically flat spacetimes, as signaled by the logarithmic correction. Except for the cases with  $n = 2, \ell = 3/2$ ,  $n = \ell = 2$  and  $n = 2, \ell = 3$ , previously studied in Refs. [87] (where a minor typo appears in Eq. (3.2)), [36], and [90], respectively, the remaining solutions appear here for the first time, to the best of our knowledge.

### 3.3 Exponentially suppressed density profiles: $\rho(r) = \rho_0 \exp[-(r/r_d)^n]$

The density function with exponential decay

$$\rho(r) = \rho_0 \exp[-(r/r_d)^n], \quad (3.40)$$

is sometimes referred to as Einasto profile [89, 91, 92] and has been extensively employed in the investigation of dark matter halos. With  $\rho_0 > 0$  and finite, conditions (2.32) hold whenever  $n > 0$ , while the central isotropy constraint (2.35a) requires  $n > 1$ . On the other hand, the DEC is always violated in this setting for  $r > r_d(4/n)^{1/n}$ .

The metric function corresponding to the *ansatz* (3.40) can be cast in terms of the incomplete Gamma function  $\Gamma(a, z)$  [85], namely

$$B(r) = 1 + \frac{c_1}{r} + \frac{\lambda r_d}{nr} \Gamma\left[3/n, (r/r_d)^n\right]. \quad (3.41)$$

In general, it is not possible to formulate  $\Gamma(a, z)$  via elementary functions. However, when  $a \equiv 3/n$  is a positive integer or half-integer, such reductions are possible (cf. Sec. 6.5 of Ref. [85]), and the relevant cases with  $n > 1$  are as follow:

- integer  $a$ :

- $a = 1 \Rightarrow n = 3$ ,
- $a = 2 \Rightarrow n = 3/2$ ,

- half-integer  $a$ :

- $a = 1/2 \Rightarrow n = 6$ ,
- $a = 3/2 \Rightarrow n = 2$ ,
- $a = 5/2 \Rightarrow n = 6/5$ .

The scenarios with integer  $a$  listed above yield purely elementary expressions, while those with half-integer  $a$  also involve the error function  $\text{erf}(z) = \frac{2}{\sqrt{\pi}} \int_0^z \exp[-t^2] dt$  (in particular, the one with  $a = 3/2$  has been recently examined in Ref. [89]). The former will be examined in Secs. 3.3.1 and 3.3.2.

#### 3.3.1 Dymnikova black hole ( $n = 3$ )

The case  $n = 3$  (i.e.,  $a = 1$ ) is particularly noteworthy. In fact, the identity

$$\Gamma(1, z) = e^{-z}, \quad (3.42)$$

with  $z \equiv (r/r_d)^3$ , gives the general solution

$$B(r) = 1 + \frac{c_1}{r} + \frac{\lambda r_d}{3r} \exp[-(r/r_d)^3]. \quad (3.43)$$

Regularity at  $r = 0$  sets the integration constant to  $c_1 = -\lambda r_d/3$ , yielding

$$B(r) = 1 - \frac{\lambda r_d}{3r} \{1 - \exp[-(r/r_d)^3]\}, \quad (3.44)$$

which reproduces the well-known Dymnikova nonsingular black hole solution [18], with effective ADM mass  $m_{\text{eff}} = \lambda r_d/6$ . Remarkably, our framework allows this geometry to arise from the unified and general density profile (3.40), rather than from the effective vacuum-polarization stress-energy adopted in Ref. [18].

### 3.3.2 New regular solutions ( $n = 3/2$ )

In the scenario with  $n = 3/2$ , we can resort to the result

$$\Gamma\left[2, (r/r_d)^{3/2}\right] = \left[(r/r_d)^{3/2} + 1\right] \exp\left[-(r/r_d)^{3/2}\right], \quad (3.45)$$

stemming from the identity  $\Gamma(2, z) = (z + 1)e^{-z}$  [85]. In this way, starting from Eq. (3.41), we find that the metric function  $B(r)$  admits the closed form

$$B(r) = 1 - \frac{2\lambda r_d}{3r} \left\{ 1 - e^{-(r/r_d)^{3/2}} \left[ (r/r_d)^{3/2} + 1 \right] \right\}, \quad (3.46)$$

where we have fixed the integration constant to  $c_1 = -2\lambda r_d/3$ . This solution exhibits a de Sitter core and is strictly asymptotically flat, with an effective ADM mass  $m_{\text{eff}} = \lambda r_d/3$ . To the best of our knowledge, this regular spacetime has never been derived in the existing literature.

### 3.4 The composite density profiles $\rho(r) = \rho_0(r/r_d)^\ell \exp[-(r/r_d)^n]$ and $\rho(r) = \rho_0(r/r_d)^\kappa [1 + (r/r_d)^n]^{-\ell}$

The power-law-modulated exponentially suppressed profile

$$\rho(r) = \rho_0 \left(\frac{r}{r_d}\right)^\ell \exp\left[-\left(\frac{r}{r_d}\right)^n\right], \quad (3.47)$$

generalizes the density function analyzed in Sec. 3.3 (see Eq. (3.40)). With this parameterization, the monotonicity assumption (2.32b) furnishes

$$\ell \leq 0, \quad n \geq 0, \quad (3.48)$$

while the finiteness requirement of  $\rho(r)$  at the origin further enforces  $\ell = 0$ , thereby reducing the model to the class discussed before.

If the energy criteria are relaxed, regular spacetimes may still be obtained for other choices of parameters, with

$$B(r) = 1 + \frac{c_1}{r} + \frac{\lambda r_d}{nr} \Gamma\left[\frac{l+3}{n}, \left(\frac{r}{r_d}\right)^n\right]. \quad (3.49)$$

For example, the regular geometries considered in Refs. [14, 38] can be identified with the choice  $\ell = -4$  and  $n = -1$ , while the model studied in Ref. [93] corresponds to  $\ell = -5$  and  $n = -2$ . However, these solutions generically violate the NEC in the vicinity of the origin and will not be considered in this paper.

We now turn our attention to the *ansatz*

$$\rho(r) = \rho_0 \left(\frac{r}{r_d}\right)^\kappa \left[ 1 + \left(\frac{r}{r_d}\right)^n \right]^{-\ell}, \quad (3.50)$$

which features the additional term  $(r/r_d)^\kappa$  compared to the power-law configuration (3.19), and represents the most complex scenario studied in this work, with  $\mathcal{C} = 8$  (see Table 1). Such profiles play an important role within the context of dark-matter halo modeling [94–97] and have also been exploited recently in the construction of regular black holes [87, 89].

Regularity at the center immediately implies <sup>3</sup>

$$\kappa \geq 0. \quad (3.51)$$

However, for  $\kappa > 0$  one has  $\rho(0) = 0$ . In this case, imposing the bound (2.32b) on  $\rho'(r)$  would inevitably force the energy density to attain negative values, unless the trivial vacuum limit is considered. Therefore, the power-law prefactor must be absent, namely  $\kappa = 0$ , in order to obtain a regular solution satisfying the WEC and possessing a finite, nonvanishing density at the origin. In this limit, the model reduces to the class examined in Sec. 3.2.

### 3.5 Superposition of regular solutions

Within the Einstein field equations (2.19), the relation for the energy density  $\rho(r)$ , which can be equivalently written as (cf. Eq. (2.19a))

$$\rho = \frac{1 - B - rB'}{8\pi r^2}, \quad (3.52)$$

is linear in the metric function  $B(r)$  and its derivative. Owing to this property, the superposition principle applies, so that any linear combination of the solutions examined before produces a new regular model whose energy density is given by the corresponding linear combination of the individual density profiles.

More precisely, let  $B_1(r)$  and  $B_2(r)$  denote two regular geometries associated with the densities  $\rho_1(r)$  and  $\rho_2(r)$ , respectively. Then

$$B(r) = a_1 B_1(r) + a_2 B_2(r) + 1 - (a_1 + a_2), \quad (3.53)$$

is also regular, and is sourced by

$$\rho(r) = a_1 \rho_1(r) + a_2 \rho_2(r), \quad (3.54)$$

with  $a_1$  and  $a_2$  arbitrary constants. The constant terms occurring on the right-hand side of Eq. (3.53) guarantee that  $B(r)$  attains the Minkowski form for  $r \rightarrow \infty$  (see Eq. (2.35b)); in addition, if the two metrics are strictly asymptotically flat and admit effective ADM masses  $m_{1,\text{eff}}$  and  $m_{2,\text{eff}}$ , the resulting spacetime remains strictly asymptotically flat, with an effective ADM mass  $a_1 m_{1,\text{eff}} + a_2 m_{2,\text{eff}}$ .

The superposition principle thus enables the systematic construction of new families of regular geometries from simpler building blocks. The generated configurations inherit key properties of the original ones, such as regularity at the center and their asymptotic behavior. As an example, by combining the rational falloff profiles with  $n = 3$  and  $n = 6$  (see Eq. (3.3))

$$\rho(r) = \rho_0 \left[ \frac{1}{1 + (r/r_d)^3} + \frac{1}{1 + (r/r_d)^6} \right], \quad (3.55)$$

---

<sup>3</sup>When  $n < 0$ , the density (3.50) behaves as  $\rho(r) \sim \rho_0 (r/r_d)^{\kappa + |n|\ell}$  near  $r = 0$ . To have a finite and non-vanishing central density, one must set  $\kappa = -|n|\ell$ , for which the profile can be recast into the simple form  $\rho(r) = \rho_0 [1 + (r/r_d)^{|n|}]^{-\ell}$ . This form is identical to the  $n > 0$  case after a redefinition of the exponent. Therefore, without loss of generality, we may restrict to  $n > 0$  and impose  $\kappa = 0$  to ensure that  $\rho(0)$  is finite and nonvanishing.

we are led to (cf. Eqs. (3.9) and (3.11))

$$B(r) = 1 - \frac{\lambda r_d}{3r} \ln\left(\frac{r^3}{r_d^3} + 1\right) - \frac{\lambda r_d}{3r} \arctan\left(\frac{r^3}{r_d^3}\right). \quad (3.56)$$

In this case, the core energy density becomes  $\rho(0) = 2\rho_0$ , and the spacetime is marginally asymptotically flat due to the logarithmic contribution.

## 4 Horizons and photon spheres

In this section we discuss, in a model-independent manner, the conditions for the existence of horizons and photon spheres in the regular spacetimes constructed in Sec. 3. These structures play a central role in gravitational lensing and black hole shadow phenomenology (see e.g. Refs. [98–107]), and determine whether a given solution represents a regular black hole (featuring both a horizon and a photon sphere), a compact object (which lacks a horizon, but possesses at least one photon sphere), or a generic horizonless regular configuration with no photon sphere.

For the static, spherically symmetric metrics of the form (2.1), horizons are located at the hypersurfaces  $r = r_h$  where their temporal component vanishes, namely

$$B(r_h) = 0. \quad (4.1)$$

If such a root is admitted and is simple,  $B'(r_h) \neq 0$ , the surface gravity is finite and the solution describes a non-extremal black hole, while degenerate scenarios satisfying  $B(r_h) = B'(r_h) = 0$  correspond to extremal cases.

In many regular black hole models,  $B(r)$  presents two distinct positive roots, giving rise to an outer (event) horizon and an inner (Cauchy) horizon [19, 108]. This causal structure is reminiscent of the (non-extremal) Reissner-Nordström geometry, where the electric charge likewise leads to a double-horizon pattern. However, spacetimes containing an inner (Cauchy) horizon are generically unstable under linear perturbations [4], and in particular the well-known mass-inflation mechanism [109, 110] implies that small perturbations can be infinitely blueshifted near the Cauchy horizon. This phenomenon causes the effective mass function to diverge, thereby converting the Cauchy horizon into a mass-inflation singularity [110]. Therefore, although the existence of two horizons is a common feature of regular black holes, their physical viability necessitates a careful stability investigation [111]. This issue lies beyond the scope of this work, but should be borne in mind when interpreting multi-horizon solutions constructed within our framework.

We now turn to the analysis of circular photon orbits, which define photon spheres. The null geodesic equation in the equatorial plane  $\theta = \pi/2$  of the spacetime (2.1) is given by

$$\dot{r}^2 + V_{\text{eff}}(r) = E^2, \quad (4.2a)$$

with

$$V_{\text{eff}}(r) = \frac{L^2}{r^2} B(r), \quad (4.2b)$$

where  $E$  and  $L$  are the conserved energy and angular momentum, respectively, and an overdot denotes differentiation with respect to the affine parameter. Circular null trajectories

correspond to special solutions of the radial dynamics (4.2) occurring at  $r = r_{\text{ph}}$ , where  $\dot{r} = 0$  and  $\partial V_{\text{eff}}/\partial r = 0$ . This yields the geometric identity

$$y(r_{\text{ph}}) := 2B(r_{\text{ph}}) - r_{\text{ph}}B'(r_{\text{ph}}) = 0, \quad (4.3)$$

which, via the mass function defined in Eq. (2.28), leads to

$$\frac{r_{\text{ph}}}{3} = m(r_{\text{ph}}) - m_{\text{loc}}(r_{\text{ph}}), \quad (4.4)$$

with

$$m_{\text{loc}}(r_{\text{ph}}) \equiv \frac{4\pi}{3} r_{\text{ph}}^3 \rho(r_{\text{ph}}). \quad (4.5)$$

The above quantity can be interpreted as the local effective mass associated with the energy density at the photon sphere radius. It represents the mass that would be contained inside a sphere of radius  $r_{\text{ph}}$  if the density were homogeneous and equal to its boundary value  $\rho(r_{\text{ph}})$ . Relation (4.4) thus shows that the existence of a photon sphere is controlled by the competition between the cumulative mass  $m(r_{\text{ph}})$  and the local effective term  $m_{\text{loc}}(r_{\text{ph}})$ . In the vacuum limit,  $\rho(r) = 0$  and  $m(r) = \text{constant} \equiv M$ , and one immediately recovers the standard Schwarzschild result  $r_{\text{ph}} = 3M$ . On the other hand, for sufficiently concentrated matter distributions,  $m(r_{\text{ph}})$  dominates over  $m_{\text{loc}}(r_{\text{ph}})$ , allowing circular null paths to exist even in the absence of horizons. In contrast, for more diffuse density profiles, the local effective contribution becomes comparable to the cumulative mass, and Eq. (4.4) may fail to admit a positive solution.

This structure highlights an important difference between the conditions defining horizons and photon spheres: while the former depend solely on the function  $2m(r)/r$ , which can be related to the compactness of a gravitating body (conventionally defined as the ratio of its mass to its characteristic radius [112]), the latter probe both the integrated mass and its radial gradient, and are therefore more sensitive to the detailed distribution of matter.

We also note that an extremal horizon for which  $B(r_h) = B'(r_h) = 0$  formally solves Eq. (4.3). However, this corresponds to a degenerate null geodesic that describes the horizon rather than a genuine photon sphere.

In Table 3, we report the horizon and photon sphere pattern of some representative regular geometries constructed in Sec. 3. Different values of  $\lambda := 8\pi\rho_0 r_d^2$  amount to distinct spacetime configurations. Denoting by  $\lambda_h$  the critical parameter determined by  $B(r) = B'(r) = 0$ , one finds that for  $\lambda > \lambda_h$  two horizons appear,  $\lambda = \lambda_h$  pertains to an extremal solution, while for  $\lambda < \lambda_h$  the spacetime is horizonless.

Similarly, the existence of photon spheres is governed by the threshold  $\lambda_{\text{ph}}$ , at which  $y(r) = 0$  and  $y'(r) = 0$  are simultaneously satisfied, with  $y$  defined in Eq. (4.3). Now, for  $\lambda > \lambda_{\text{ph}}$  two photon spheres are present (in this case, if horizon(s) exists, the physically relevant photon sphere is the outer one, for which  $r_{\text{ph}} > r_h$ ), whereas  $\lambda = \lambda_{\text{ph}}$  marks the degenerate situation where the two photon spheres merge, and finally no photon sphere exists for  $\lambda < \lambda_{\text{ph}}$ .

A particularly interesting regime arises when  $\lambda_{\text{ph}} \leq \lambda < \lambda_h$ . This parameter window describes regular horizonless geometries bearing at least one circular null orbit, which typically represents an outer unstable photon sphere. These features typically qualify compact objects that can potentially mimic several optical properties of black holes [100, 113], as the presence of a photon sphere leads to strong light bending and can produce observational signatures such as a shadow-like dark region in gravitational lensing images.



Reference	Metric function $B(x)$	Horizon	Photon sphere
Eq. (3.9)	$1 - \frac{\lambda}{3x} \ln(x^3 + 1)$	$\lambda_h \approx 2.66816$ $r_h^{\text{crit}} \approx 2.50935 r_d$	$\lambda_{\text{ph}} \approx 2.49566$ $r_{\text{ph}}^{\text{crit}} \approx 3.58630 r_d$
Eq. (3.11)	$1 - \frac{\lambda}{3x} \arctan(x^3)$	$\lambda_h \approx 3.41005$ $r_h^{\text{crit}} \approx 1.29517 r_d$	$\lambda_{\text{ph}} \approx 2.89399$ $r_{\text{ph}}^{\text{crit}} \approx 1.67954 r_d$
Eq. (3.37)	$1 - \frac{2\lambda}{3(\ell-2)(\ell-1)x} \times$ $\left[ 1 - \frac{(\ell-1)x^3 + \ell x^{3/2} + 1}{(1+x^{3/2})^\ell} \right]$	$\ell = \frac{8}{3} : \lambda_h \approx 8.53347$ $r_h^{\text{crit}} \approx 1.89547 r_d$	$\ell = \frac{8}{3} : \lambda_{\text{ph}} \approx 7.87271$ $r_{\text{ph}}^{\text{crit}} \approx 2.76737 r_d$
		$\ell = 3 : \lambda_h \approx 10.715$ $r_h^{\text{crit}} \approx 1.5874 r_d$	$\ell = 3 : \lambda_{\text{ph}} \approx 9.79886$ $r_{\text{ph}}^{\text{crit}} \approx 2.30522 r_d$
		$\ell = 4 : \lambda_h \approx 17.8882$ $r_h^{\text{crit}} \approx 1.10545 r_d$	$\ell = 4 : \lambda_{\text{ph}} \approx 16.0724$ $r_{\text{ph}}^{\text{crit}} \approx 1.5874 r_d$
		$\ell = 5 : \lambda_h \approx 25.8547$ $r_h^{\text{crit}} \approx 0.872071 r_d$	$\ell = 5 : \lambda_{\text{ph}} \approx 22.9836$ $r_{\text{ph}}^{\text{crit}} \approx 1.24345 r_d$
		$\ell = 6 : \lambda_h \approx 34.4839$ $r_h^{\text{crit}} \approx 0.731391 r_d$	$\ell = 6 : \lambda_{\text{ph}} \approx 30.436$ $r_{\text{ph}}^{\text{crit}} \approx 1.03782 r_d$
		$\ell = 7 : \lambda_h \approx 43.6879$ $r_h^{\text{crit}} \approx 0.636061 r_d$	$\ell = 7 : \lambda_{\text{ph}} \approx 38.3623$ $r_{\text{ph}}^{\text{crit}} \approx 0.899367 r_d$
		Eq. (3.46)	$1 - \frac{2\lambda}{3x} \left[ 1 - e^{-x^{3/2}} (x^{3/2} + 1) \right]$
Table 2 ( $n = 2, \ell = 7/2$ )	$1 - \frac{\lambda x^2(5+2x^2)}{15(x^2+1)^{5/2}}$	$\lambda_h \approx 12.1034$ $r_h^{\text{crit}} \approx 1.04377 r_d$	$\lambda_{\text{ph}} \approx 10.6195$ $r_{\text{ph}}^{\text{crit}} \approx 1.45467 r_d$
Table 2 ( $n = 6, \ell = 5/2$ )	$1 - \frac{\lambda x^2(2x^6+3)}{9(x^6+1)^{3/2}}$	$\lambda_h \approx 5.086$ $r_h^{\text{crit}} \approx 0.980029 r_d$	$\lambda_{\text{ph}} \approx 4.03397$ $r_{\text{ph}}^{\text{crit}} \approx 1.2044 r_d$

**Table 3:** Horizon and photon sphere structure for selected regular spacetimes introduced in Sec. 3. For each metric function  $B(x)$  (with  $x := r/r_d$ ), we report the critical values  $\lambda_h$  and  $\lambda_{\text{ph}}$  of  $\lambda := 8\pi\rho_0 r_d^2$ , together with the associated critical radii  $r_h^{\text{crit}}$  and  $r_{\text{ph}}^{\text{crit}}$ . The parameters  $\lambda_h$  and  $\lambda_{\text{ph}}$  are set by the conditions  $B(r) = B'(r) = 0$  and  $y(r) = y'(r) = 0$  (cf. Eq. (4.3)), respectively, with the former controlling the emergence of horizons and the latter that of photon spheres. Two horizons ( $\lambda > \lambda_h$ ), an extremal configuration ( $\lambda = \lambda_h$ ) at  $r = r_h^{\text{crit}}$ , where the two horizons coincide, or no horizon ( $\lambda < \lambda_h$ ) can occur. Similarly, the spacetime can feature two photon spheres ( $\lambda > \lambda_{\text{ph}}$ ), a degenerate scenario ( $\lambda = \lambda_{\text{ph}}$ ) at  $r = r_{\text{ph}}^{\text{crit}}$ , or no photon sphere ( $\lambda < \lambda_{\text{ph}}$ ).

## 5 Junction conditions

In this section, we examine whether the regular solutions derived in Sec. 3 can be matched, at some finite radius  $r = r_* > 2M$ , to a Schwarzschild exterior

$$ds_{\text{Schw}}^2 = -f(r) dt^2 + f^{-1}(r) dr^2 + r^2 d\Omega^2, \quad (5.1a)$$

with

$$f(r) \equiv 1 - \frac{2M}{r}. \quad (5.1b)$$

To this end, we employ the well-known Darmois-Israel formalism [12, 75, 114–117], which establishes that the junction conditions for a smooth joining of two spacetimes across a non-null hypersurface  $\Sigma$  can be formulated, in a coordinate-independent way, as

$$[h_{AB}] = 0, \quad (5.2)$$

$$[K_{AB}] = 0, \quad (5.3)$$

the square brackets denoting the jump across the hypersurface. Matching relations then enforce continuity across  $\Sigma$  of the induced metric  $h_{AB}$  and the extrinsic curvature  $K_{AB}$ , where capital Latin indices label intrinsic coordinates on  $\Sigma$ .

In Sec. 5.1, we prove that a smooth  $C^1$  matching to the Schwarzschild geometry (5.1) is impossible at any finite radius  $r = r_*$ , and hence the appearance of a thin shell is unavoidable, as discussed in Sec. 5.2.

### 5.1 Impossibility of a smooth matching

We recall that in Eq. (2.28) we have expressed the metric component  $B(r)$  underlying the family of Kerr-Schild spacetimes (2.1) in terms of the Misner-Sharp-Hernandez mass  $m(r)$ . For the regular models constructed in this paper, such mass function complies with

$$m(0) = 0, \quad (5.4a)$$

$$m'(r) > 0 \quad \text{for all finite } r > 0. \quad (5.4b)$$

Assume now, for contradiction, that at some  $r = r_* > 0$  both the first and second junction conditions (5.2) and (5.3) are valid, thereby implying

$$B(r_*) = f(r_*), \quad (5.5)$$

$$B'(r_*) = f'(r_*). \quad (5.6)$$

From the first identity, we obtain

$$m(r_*) = M, \quad (5.7)$$

which, when plugged into the second, yields

$$\frac{2M}{r_*^2} - \frac{2m'(r_*)}{r_*} = \frac{2M}{r_*^2} \implies m'(r_*) = 0. \quad (5.8)$$

Since this relation contradicts property (5.4b), no smooth matching to the Schwarzschild exterior can occur, as claimed. Although our argument holds for any finite  $r_* > 0$ , our interest is restricted to  $r_* > 2M$ .

## 5.2 Formation of a thin shell

From the analysis of the previous section, it follows that regular spacetimes of form (2.1) can be matched to a Schwarzschild exterior only by allowing for a thin shell of matter outside the Schwarzschild horizon, namely at  $r = r_* > 2M$ .

In this scenario, the first junction condition (5.5) is imposed, while the second, Eq. (5.6), is relaxed. Accordingly, the Darmois-Israel formalism predicts the emergence of a surface layer with stress-energy tensor [75],

$$S_{AB} = -\frac{1}{8\pi} ([K_{AB}] - h_{AB}[K]), \quad (5.9)$$

with  $[K] = [h^{AB}K_{AB}]$ . Physically,  $[K_{AB}]$  accounts for the discontinuity in the radial gradient of the gravitational potential across the junction surface  $r = r_*$ .

It is not difficult to prove that  $S^A_B$  takes the diagonal perfect-fluid form [12, 75]

$$S^A_B = \text{diag}(-\sigma, \mathcal{P}, \mathcal{P}), \quad (5.10)$$

where  $\sigma$  and  $\mathcal{P}$  are the surface energy density and pressure, respectively. In our setup, these quantities read as

$$\sigma = -\frac{1}{4\pi r_*} \left( \sqrt{f(r_*)} - \sqrt{B(r_*)} \right), \quad (5.11)$$

$$\mathcal{P} = \frac{1}{16\pi} \left( \frac{f'(r_*)}{\sqrt{f(r_*)}} - \frac{B'(r_*)}{\sqrt{B(r_*)}} \right). \quad (5.12)$$

As a consequence of the first matching relation (5.5), we have

$$\sigma = 0, \quad (5.13)$$

while the tangential pressure remains nonvanishing:

$$\mathcal{P} = \frac{f'(r_*) - B'(r_*)}{16\pi\sqrt{B(r_*)}} = \frac{m'(r_*)}{8\pi r_*} \frac{1}{\sqrt{1 - 2M/r_*}}, \quad (5.14)$$

where we used Eq. (2.28) jointly with identity (5.7).

Therefore, within our hypotheses, the matching entails a surface layer endowed with a *positive*  $\mathcal{P}$ . In view of Eq. (5.13), this indicates that the DEC is spoiled, while the remaining energy criteria hold.

## 6 Concluding remarks

In this paper, we have devised a method for constructing families of static, spherically symmetric regular spacetimes in general relativity satisfying the WEC.

The starting point of our construction is given by the WEC requirements (2.26a) and (2.26b), jointly with the regularity assumption (2.26c), the latter only calling for the boundedness of a single invariant, namely the Kretschmann scalar. Remarkably, this condition guarantees the finiteness of all curvature invariants, including the full set of Zakhary-McIntosh scalars, and is equivalent to causal geodesic completeness for all the configurations studied in this paper, which display asymptotically Minkowskian behavior and regular cores.

Hypotheses (2.26) translate into the system of ordinary differential equations (2.29)–(2.31), supplemented by the admissibility criteria (2.32) and (2.35) encoding physically reasonable regularity, boundary, and monotonicity conditions on the matter distribution and the metric function  $B(r)$ . In this way, regular WEC-obeying solutions can be immediately obtained by solving Eq. (2.19a), which relates  $B(r)$  and the energy density  $\rho(r)$  via a linear differential equation (see Sec. 2).

The validity of the WEC provides a physical basis for the spacetimes derived within our scheme, which we have studied in detail in Sec. 3 by classifying energy-density profiles in terms of their complexity parameter  $\mathcal{C}$ . Well-known regular models, such as the Bardeen, Hayward, and Dymnikova geometries, or prominent dark-matter halo paradigms, emerge as particular realizations of a broader and unified framework, where closed-form expressions for new regular solutions can also be computed (see, e.g., Eqs. (3.11), (3.37), and (3.46), and Table 2). These may represent, depending on the presence of horizons and photon spheres, geometric candidates for either black holes or generic compact objects (see Sec. 4), and satisfy consistent junction conditions (see Sec. 5). However, key aspects such as stability and formation scenarios have not been addressed, and hence the astrophysical relevance of the new solutions remains to be established.

Our analysis has involved energy densities  $\rho(r)$  with a relatively simple analytic structure, as reflected by the fact that they are characterized by  $\mathcal{C} \leq 8$ . If no further profiles with lower complexity can be identified, it is plausible to conclude that we have explored the simplest choices for  $\rho(r)$  that lead to regular spacetimes adhering to the WEC. Nevertheless, our systematic approach can be extended to general models with more complicated structures. In addition, it allows us to study a broader class of nonsingular configurations, including, for example, wormholes [118–123], gravastar-like structures [124–127], or generic exotic compact objects [100]. Although such extensions have not been explicitly realized here, it is likely that they could avoid singular behavior while satisfying relevant energy conditions through suitably chosen matter distributions or regularization schemes. Assessing the viability and physical consistency of such hypothetical scenarios constitutes an interesting avenue for future work.

In this regard, a subtle issue concerning regularity should be mentioned. In Ref. [128], seven criteria have been proposed to determine physically reasonable nonsingular black holes. Configurations such as Bardeen, Hayward, Dymnikova, Fan-Wang, and their rotating counterparts were found not to fulfill all of them simultaneously (see, e.g., Table 5 in Ref. [128]). This highlights that the study of regular metrics represents an active area of research deserving further investigation.

## Acknowledgments

The work of Z. W. is supported by the National Natural Science Foundation of China (12405063). E. B. acknowledges the support of INFN *iniziativa specifica* Moonlight2.

## A Riemann tensor components and Zakhary-McIntosh invariants

In this Appendix, we compute the components of the Riemann tensor and the full set of the Zakhary-McIntosh (ZM) invariants for the static, spherically symmetric geometry (2.1). These computations are most conveniently carried out in an orthonormal basis [4], using the tetrad field defined in Eq. (2.17).

The torsion-free condition, also known as the first Cartan structure equation [4], can be written in the language of differential forms as [74, 129]

$$de^a + \omega^a_b \wedge e^b = 0, \quad (\text{A.1})$$

where  $e^a = e^a_\mu dx^\mu$  denotes the orthonormal coframe,  $\omega^a_b$  the spin connection one-form, and frame indices  $a, b, \dots = \hat{0}, \hat{1}, \hat{2}, \hat{3}$ . For the metric (2.1), the nonvanishing components of the spin connection are then found to be

$$\omega^{\hat{0}}_{\hat{1}} = -\omega^{\hat{1}}_{\hat{0}} = \frac{B'}{2} dt = \frac{B'}{2\sqrt{B}} e^{\hat{0}}, \quad (\text{A.2a})$$

$$\omega^{\hat{1}}_{\hat{2}} = -\omega^{\hat{2}}_{\hat{1}} = -\sqrt{B} d\theta = -\frac{\sqrt{B}}{r} e^{\hat{2}}, \quad (\text{A.2b})$$

$$\omega^{\hat{1}}_{\hat{3}} = -\omega^{\hat{3}}_{\hat{1}} = -\sqrt{B} \sin\theta d\phi = -\frac{\sqrt{B}}{r} e^{\hat{3}}, \quad (\text{A.2c})$$

$$\omega^{\hat{2}}_{\hat{3}} = -\omega^{\hat{3}}_{\hat{2}} = -\cos\theta d\phi = -\frac{\cot\theta}{r} e^{\hat{3}}, \quad (\text{A.2d})$$

where we recall that a prime denotes the differentiation with respect to the radial variable  $r$ . The curvature two-form can be obtained from the second Cartan structure equation

$$R^a_b = d\omega^a_b + \omega^a_c \wedge \omega^c_b. \quad (\text{A.3})$$

Then, employing Eq. (A.2), we obtain the following nonvanishing components of  $R^a_b$ :

$$R^{\hat{0}}_{\hat{1}} = -R^{\hat{1}}_{\hat{0}} = \frac{B''}{2} dr \wedge dt = \frac{B''}{2} e^{\hat{1}} \wedge e^{\hat{0}}, \quad (\text{A.4a})$$

$$R^{\hat{0}}_{\hat{2}} = -R^{\hat{2}}_{\hat{0}} = -\frac{\sqrt{B}B'}{2} dt \wedge d\theta = -\frac{B'}{2r} e^{\hat{0}} \wedge e^{\hat{2}}, \quad (\text{A.4b})$$

$$R^{\hat{0}}_{\hat{3}} = -R^{\hat{3}}_{\hat{0}} = -\frac{\sqrt{B}B' \sin\theta}{2} dt \wedge d\phi = -\frac{B'}{2r} e^{\hat{0}} \wedge e^{\hat{3}}, \quad (\text{A.4c})$$

$$R^{\hat{1}}_{\hat{2}} = -R^{\hat{2}}_{\hat{1}} = -\frac{B'}{2\sqrt{B}} dr \wedge d\theta = -\frac{B'}{2r} e^{\hat{1}} \wedge e^{\hat{2}}, \quad (\text{A.4d})$$

$$R^{\hat{1}}_{\hat{3}} = -R^{\hat{3}}_{\hat{1}} = -\frac{B' \sin\theta}{2\sqrt{B}} dr \wedge d\phi = -\frac{B'}{2r} e^{\hat{1}} \wedge e^{\hat{3}}, \quad (\text{A.4e})$$

$$R^{\hat{2}}_{\hat{3}} = -R^{\hat{3}}_{\hat{2}} = (1-B) \sin\theta d\theta \wedge d\phi = \frac{1-B}{r^2} e^{\hat{2}} \wedge e^{\hat{3}}. \quad (\text{A.4f})$$

It is thus evident that the curvature two-form involves only three independent functions of  $r$ , namely (cf. Eq. (2.5))

$$X(r) := \frac{B''}{2}, \quad Y(r) := \frac{B'}{2r}, \quad Z(r) := \frac{1-B}{r^2}. \quad (\text{A.5})$$

Now, from the definition of the curvature two-form [74]

$$R^a_b := \frac{1}{2} R^a_{bcd} e^c \wedge e^d, \quad (\text{A.6})$$

one can directly read off the following independent nonvanishing components of the Riemann tensor in the orthonormal frame:

$$R_{\hat{0}\hat{1}\hat{0}\hat{1}} = X, \quad (\text{A.7a})$$

$$R_{\hat{0}\hat{2}\hat{0}\hat{2}} = R_{\hat{0}\hat{3}\hat{0}\hat{3}} = Y, \quad (\text{A.7b})$$

$$R_{\hat{1}\hat{2}\hat{1}\hat{2}} = R_{\hat{1}\hat{3}\hat{1}\hat{3}} = -Y, \quad (\text{A.7c})$$

$$R_{\hat{2}\hat{3}\hat{2}\hat{3}} = Z, \quad (\text{A.7d})$$

all the other nonvanishing components following from the usual symmetries

$$R_{abcd} = -R_{bacd} = -R_{abdc} = R_{cdab}. \quad (\text{A.8})$$

Because the frame indices are raised and lowered with the Minkowski metric  $\eta_{ab} = \text{diag}(-1, 1, 1, 1)$ , the full set of Riemann tensor components—irrespective of index positions—is algebraically determined by the three functions (A.5). Consequently, *all* algebraic curvature invariants constructed by complete contractions of Riemann tensor, such as the Kretschmann and Ricci scalars, or the other higher-order ZM invariants, can be expressed as polynomials in  $X(r)$ ,  $Y(r)$ , and  $Z(r)$  with constant coefficients. Although this result is derived in an orthonormal frame, it is completely general, since curvature scalars are independent of the choice of the coordinates.

Therefore, the condition that the three basic curvature functions  $X$ ,  $Y$ , and  $Z$  remain finite, is both necessary and sufficient to guarantee that *all* algebraic curvature invariants of the spacetime are finite. Thus, considering in particular the center  $r = 0$  and assuming that  $B(r)$  admits the power-series expansion

$$B(r) = B_0 + B_1 r + B_2 r^2 + \mathcal{O}(r^3), \quad (\text{A.9})$$

it follows from Eq. (A.5) that the finiteness of  $X$ ,  $Y$ , and  $Z$  as  $r \rightarrow 0$  requires

$$B_0 = 1, \quad B_1 = 0, \quad (\text{A.10})$$

as we have already shown in Eq. (2.8). Conversely, if Eq. (A.10) holds, then  $X$ ,  $Y$ , and  $Z$  remain finite at the origin. Therefore, Eq. (A.10) provides a necessary and sufficient condition for the boundedness of all algebraic curvature invariants at  $r = 0$ .

For completeness, we now derive the whole set of the seventeen ZM invariants [130–132] for the metric (2.1). For this reason, we introduce the Weyl tensor, defined as the trace-free part of the Riemann tensor [4]

$$C_{abcd} = R_{abcd} - \frac{1}{2}(g_{ac}R_{bd} - g_{ad}R_{bc} - g_{bc}R_{ad} + g_{bd}R_{ac}) + \frac{R}{6}(g_{ac}g_{bd} - g_{ad}g_{bc}), \quad (\text{A.11})$$

where  $g_{ab} = \eta_{ab}$  in an orthonormal frame. A direct computation yields the independent nonvanishing components

$$C_{\hat{0}\hat{1}\hat{0}\hat{1}} = \frac{1}{3}(X - 2Y - Z), \quad (\text{A.12a})$$

$$C_{\hat{0}\hat{2}\hat{0}\hat{2}} = C_{\hat{0}\hat{3}\hat{0}\hat{3}} = \frac{1}{6}(-X + 2Y + Z), \quad (\text{A.12b})$$

$$C_{\hat{1}\hat{2}\hat{1}\hat{2}} = C_{\hat{1}\hat{3}\hat{1}\hat{3}} = \frac{1}{6}(X - 2Y - Z), \quad (\text{A.12c})$$

$$C_{\hat{2}\hat{3}\hat{2}\hat{3}} = \frac{1}{3}(-X + 2Y + Z). \quad (\text{A.12d})$$

We find that the nonvanishing ZM invariants for the spacetime (2.1) are given by <sup>4</sup>

$$\mathcal{I}_1 := C_{abcd} C^{abcd} = \frac{4}{3}(-X + 2Y + Z)^2, \quad (\text{A.13a})$$

$$\mathcal{I}_3 := C_{ab}{}^{cd} C_{cd}{}^{ef} C_{ef}{}^{ab} = -\frac{4}{9}(X - 2Y - Z)^3, \quad (\text{A.13b})$$

$$\mathcal{I}_5 := R = 2(Z - X - 4Y), \quad (\text{A.13c})$$

$$\mathcal{I}_6 := R_{ab} R^{ab} = 2(X + 2Y)^2 + 2(2Y - Z)^2, \quad (\text{A.13d})$$

$$\mathcal{I}_7 := R^a{}_b R^b{}_c R^c{}_a = 2[(Z - 2Y)^3 - (X + 2Y)^3], \quad (\text{A.13e})$$

$$\mathcal{I}_8 := R^a{}_b R^b{}_c R^c{}_d R^d{}_a = 2[(X + 2Y)^4 + (Z - 2Y)^4], \quad (\text{A.13f})$$

$$\mathcal{I}_9 := C_{abcd} R^{bc} R^{ad} = \frac{2}{3}(X + Z)^2(X - 2Y - Z), \quad (\text{A.13g})$$

$$\mathcal{I}_{11} := R^{ab} R^{cd} (C_{eab}{}^f C_{fcd}{}^e - {}^*C_{eab}{}^f {}^*C_{fcd}{}^e) = \frac{4}{9}(X + Z)^2(-X + 2Y + Z)^2, \quad (\text{A.13h})$$

$$\mathcal{I}_{13} := R_a{}^c R_c{}^e R_b{}^d R_d{}^f C^{ab}{}_{ef} = -\frac{2}{3}(X + Z)^2(X - 2Y - Z)(X + 4Y - Z)^2, \quad (\text{A.13i})$$

$$\mathcal{I}_{15} := \frac{1}{16} R^{ab} R^{cd} (C_{eabf} C^e{}_{cd}{}^f + {}^*C_{eabf} {}^*C^e{}_{cd}{}^f) = \frac{1}{36}(X + Z)^2(-X + 2Y + Z)^2, \quad (\text{A.13j})$$

$$\begin{aligned} \mathcal{I}_{16} &:= \frac{1}{32} R^{ab} R^{cd} C^{efgh} (C_{eabh} C_{fcdg} + {}^*C_{eabh} {}^*C_{fcdg}) \\ &= -\frac{1}{108}(X + Z)^2(X - 2Y - Z)^3, \end{aligned} \quad (\text{A.13k})$$

where  ${}^*C_{abcd}$  is the dual of the Weyl tensor

$${}^*C_{abcd} := \frac{1}{2} E_{abef} C^{ef}{}_{cd}, \quad (\text{A.14})$$

with  $E_{abef}$  the Levi-Civita tensor [131].

For completeness, we also list the remaining ZM invariants

$$\mathcal{I}_2 := {}^*C_{abcd} C^{abcd}, \quad (\text{A.15a})$$

$$\mathcal{I}_4 := C_{ab}{}^{cd} {}^*C_{cd}{}^{ef} C_{ef}{}^{ab}, \quad (\text{A.15b})$$

$$\mathcal{I}_{10} := {}^*C_{abc}{}^d R^{bc} R_d{}^a, \quad (\text{A.15c})$$

$$\mathcal{I}_{12} := 2R^{ab} R_{cd} C_{eabf} {}^*C^{ecd}{}^f, \quad (\text{A.15d})$$

$$\mathcal{I}_{14} := R_a{}^c R_c{}^e R_b{}^d R_d{}^f {}^*C^{ab}{}_{ef}, \quad (\text{A.15e})$$

$$\mathcal{I}_{17} := \frac{1}{32} R^{ab} R^{cd} {}^*C^{efgh} (C_{eabh} C_{fcdg} + {}^*C_{eabh} {}^*C_{fcdg}). \quad (\text{A.15f})$$

For the static spherically symmetric geometry (2.1), the Weyl tensor is purely electric [133], as is manifest from Eq. (A.12). Hence all parity-odd dual contractions entering the ZM scalars listed in Eq. (A.15) vanish identically.

Remarkably, the Kretschmann scalar can be expressed as

$$K = 4(X^2 + 4Y^2 + Z^2), \quad (\text{A.16})$$

<sup>4</sup>There is a typo in Eq. (6c) of Ref. [54]. Using the notations of Ref. [54], the correct expression should read  $\mathcal{I}_{13} = \frac{2}{3} \mathcal{A}_3 (\mathcal{A}_2^2 - \mathcal{A}_1^2)^2$ .

which constitutes a positive-definite quadratic form in  $X, Y$ , and  $Z$ . Consequently, the finiteness of  $K$  ensures that  $X, Y$ , and  $Z$  remain finite, and hence all other algebraic curvature invariants, including the full ZM set, are finite as well. Hence, the Kretschmann scalar *alone* is sufficient to fully determine the curvature regularity of the spacetime (2.1).

We can thus conclude that all solutions presented in Sec. 3 have finite curvature invariants. This follows, among the assumptions underlying our procedure, from hypothesis (2.32c), which, jointly with Eq. (2.35b), guarantees that  $X, Y$ , and  $Z$  remain finite for any value of  $r$ .

## B Kretschmann scalar for generic static, spherically symmetric spacetimes

In this Appendix, we show that the Kretschmann scalar *alone* is sufficient to characterize the finiteness of all curvature scalars also for a generic static, spherically symmetric spacetime [4, 12, 134]

$$ds^2 = -B(r) dt^2 + A(r) dr^2 + r^2 d\Omega^2. \quad (\text{B.1})$$

Following a procedure similar to that adopted in Sec. A, one finds the following independent nonvanishing components of the Riemann tensor in an orthonormal frame:<sup>5</sup>

$$R_{\hat{0}\hat{1}\hat{0}\hat{1}} = X_1, \quad (\text{B.2a})$$

$$R_{\hat{0}\hat{2}\hat{0}\hat{2}} = R_{\hat{0}\hat{3}\hat{0}\hat{3}} = X_2, \quad (\text{B.2b})$$

$$R_{\hat{1}\hat{2}\hat{1}\hat{2}} = R_{\hat{1}\hat{3}\hat{1}\hat{3}} = X_3, \quad (\text{B.2c})$$

$$R_{\hat{2}\hat{3}\hat{2}\hat{3}} = X_4, \quad (\text{B.2d})$$

with

$$X_1(r) := \frac{(B'/\sqrt{AB})'}{2\sqrt{AB}}, \quad X_2(r) := \frac{B'}{2rAB}, \quad X_3(r) := \frac{A'}{2rA^2}, \quad X_4(r) := \frac{1 - 1/A}{r^2}. \quad (\text{B.3})$$

The remaining components again follow from the standard symmetries (A.8) of the Riemann tensor. Consequently, any algebraic scalar invariant can be expressed as a polynomial function of  $X_1, X_2, X_3$ , and  $X_4$ . In particular, the Kretschmann scalar takes the compact form

$$K = 4(X_1^2 + 2X_2^2 + 2X_3^2 + X_4^2). \quad (\text{B.4})$$

This decomposition shows explicitly that  $K$  is a positive-definite quadratic form in  $X_1, X_2, X_3$ , and  $X_4$ . Its finiteness thus guarantees the finiteness of all algebraic curvature invariants for the generic geometry (B.1), mirroring the one-function setup studied in Appendix A. Our analysis agrees with the observation made in Refs. [135, 136]<sup>6</sup>.

<sup>5</sup>The orthonormal frame in this case can be found, for example, in Sec. 6.1 of Ref. [4].

<sup>6</sup>After completing the calculation presented in this appendix, we became aware that a decomposition of the Kretschmann scalar into a positive semi-definite sum of squares had already appeared in the literature; see, e.g., Refs. [135, 137]. With this decomposition, it follows that, in static and spherically symmetric settings, the finiteness of the Kretschmann scalar is sufficient to ensure that all algebraic curvature invariants remain finite [135, 136].



## C Evaluation of the hypergeometric function $F(1, 3/4; 7/4; -r^4/r_d^4)$

In Sec. 3.1, we have seen that the energy density (3.3) sources the geometry (3.5) involving the Gauss hypergeometric function  $F[1, 3/n; 1 + 3/n; -(r/r_d)^n]$ . Starting from the Euler integral formula [85]

$$F(a, b; c; z) = \frac{\Gamma(c)}{\Gamma(b)\Gamma(c-b)} \int_0^1 \frac{t^{b-1} (1-t)^{c-b-1}}{(1-zt)^a} dt, \quad (\text{C.1})$$

with  $\Gamma(z)$  the Euler gamma function, one recovers for  $n = 4$  the integral representation

$$F(1, 3/4; 7/4; -z) = \frac{3}{4} \int_0^1 \frac{t^{-1/4}}{1+tz} dt, \quad z \equiv (r/r_d)^4. \quad (\text{C.2})$$

Via the change of variables  $u = t^{1/4} r/r_d$ , one obtains from Eq. (C.2) the result (3.15), which we report here for convenience:

$$F[1, 3/4; 7/4; -(r/r_d)^4] = 3 \left(\frac{r_d}{r}\right)^3 I(r), \quad (\text{C.3a})$$

$$I(r) := \int_0^{r/r_d} \frac{u^2}{1+u^4} du. \quad (\text{C.3b})$$

In this appendix, we explain how  $I(r)$  can be evaluated.

Since the integrand admits the partial-fraction decomposition

$$\frac{u^2}{1+u^4} = \frac{1}{2\sqrt{2}} \left( \frac{u}{u^2 - \sqrt{2}u + 1} - \frac{u}{u^2 + \sqrt{2}u + 1} \right), \quad (\text{C.4})$$

Eq. (C.3b) can be expressed as a combination of integrals

$$I_{\pm} = \int \frac{u}{u^2 \pm \sqrt{2}u + 1} du. \quad (\text{C.5})$$

Each  $I_{\pm}$  can be split into two elementary contributions

$$I_{\pm} = \frac{1}{2} \int \frac{2u \pm \sqrt{2}}{u^2 \pm \sqrt{2}u + 1} du - \frac{\sqrt{2}}{2} \int \frac{1}{u^2 \pm \sqrt{2}u + 1} du, \quad (\text{C.6})$$

and the first term yields a logarithm

$$\int \frac{2u \pm \sqrt{2}}{u^2 \pm \sqrt{2}u + 1} du = \ln(u^2 \pm \sqrt{2}u + 1), \quad (\text{C.7})$$

while the second gives, after completing the square  $u^2 \pm \sqrt{2}u + 1 = (u \pm \frac{\sqrt{2}}{2})^2 + \frac{1}{2}$ , an arctangent

$$\int \frac{1}{u^2 \pm \sqrt{2}u + 1} du = \sqrt{2} \arctan(\sqrt{2}u \pm 1). \quad (\text{C.8})$$

Assembling the pieces, the integral (C.3b) becomes

$$I(r) = \frac{1}{2\sqrt{2}} \left\{ \arctan[\sqrt{2}(r/r_d) + 1] + \arctan[\sqrt{2}(r/r_d) - 1] \right\} + \frac{1}{4\sqrt{2}} \ln \left[ \frac{(r/r_d)^2 - \sqrt{2}(r/r_d) + 1}{(r/r_d)^2 + \sqrt{2}(r/r_d) + 1} \right]. \quad (\text{C.9})$$

This is precisely the formula given in Eq. (3.16), which leads to the regular and strictly asymptotically flat spacetime (3.17).

## References

- [1] E. Lifshitz and I. Khalatnikov, *Investigations in relativistic cosmology*, *Advances in Physics* **12** (1963) 185.
- [2] S.W. Hawking and G.F.R. Ellis, *The Large Scale Structure of Space-Time*, Cambridge Monographs on Mathematical Physics, Cambridge University Press (2, 2023), [10.1017/9781009253161](https://doi.org/10.1017/9781009253161).
- [3] S.W. Hawking, *THE PATH INTEGRAL APPROACH TO QUANTUM GRAVITY*, in *General Relativity: An Einstein Centenary Survey*, pp. 746–789 (1980).
- [4] R.M. Wald, *General Relativity*, Chicago Univ. Pr., Chicago, USA (1984), [10.7208/chicago/9780226870373.001.0001](https://doi.org/10.7208/chicago/9780226870373.001.0001).
- [5] R. Penrose, *Gravitational collapse and space-time singularities*, *Phys. Rev. Lett.* **14** (1965) 57.
- [6] S.W. Hawking and R. Penrose, *The Singularities of gravitational collapse and cosmology*, *Proc. Roy. Soc. Lond. A* **314** (1970) 529.
- [7] J.M.M. Senovilla, *Singularity Theorems and Their Consequences*, *Gen. Rel. Grav.* **30** (1998) 701 [[1801.04912](https://arxiv.org/abs/1801.04912)].
- [8] H.K. Mohajan, *Singularities in global hyperbolic space-time manifold*, *Apex Journal of Advanced Sciences & Engineering* **5** (2016) 41.
- [9] E. Curiel, *A Primer on Energy Conditions*, *Einstein Stud.* **13** (2017) 43 [[1405.0403](https://arxiv.org/abs/1405.0403)].
- [10] P. Martin-Moruno and M. Visser, *Classical and semi-classical energy conditions*, *Fundam. Theor. Phys.* **189** (2017) 193 [[1702.05915](https://arxiv.org/abs/1702.05915)].
- [11] M.S. Morris and K.S. Thorne, *Wormholes in space-time and their use for interstellar travel: A tool for teaching general relativity*, *Am. J. Phys.* **56** (1988) 395.
- [12] M. Visser, *Lorentzian Wormholes. From Einstein to Hawking*, Springer, New York, USA (1995).
- [13] C. Bambi, ed., *Regular Black Holes. Towards a New Paradigm of Gravitational Collapse*, Springer Series in Astrophysics and Cosmology, Springer (2023), [10.1007/978-981-99-1596-5](https://doi.org/10.1007/978-981-99-1596-5), [[2307.13249](https://arxiv.org/abs/2307.13249)].
- [14] C. Lan, H. Yang, Y. Guo and Y.-G. Miao, *Regular Black Holes: A Short Topic Review*, *Int. J. Theor. Phys.* **62** (2023) 202 [[2303.11696](https://arxiv.org/abs/2303.11696)].
- [15] M. Myszkowski, M. Damia Paciarini, F. Sannino and V. Vellucci, *Regular spacetimes in the effective metric description*, *Eur. Phys. J. C* **86** (2026) 346 [[2506.12620](https://arxiv.org/abs/2506.12620)].
- [16] R. Carballo-Rubio et al., *Towards a non-singular paradigm of black hole physics*, *JCAP* **05** (2025) 003 [[2501.05505](https://arxiv.org/abs/2501.05505)].
- [17] J.M. Bardeen, *Non-singular general-relativistic gravitational collapse*, in *Proc. Int. Conf. GR5, Tbilisi*, vol. 174, p. 174, sn, 1968.
- [18] I. Dymnikova, *Vacuum nonsingular black hole*, *Gen. Rel. Grav.* **24** (1992) 235.
- [19] S.A. Hayward, *Formation and evaporation of regular black holes*, *Phys. Rev. Lett.* **96** (2006) 031103 [[gr-qc/0506126](https://arxiv.org/abs/gr-qc/0506126)].
- [20] V.P. Frolov and A. Zelnikov, *Quantum radiation from an evaporating nonsingular black hole*, *Phys. Rev. D* **95** (2017) 124028 [[1704.03043](https://arxiv.org/abs/1704.03043)].
- [21] H. Liu, X. Liao and Y. Zhang, *Breaking the degeneracy among regular black holes with gravitational lensing*, [2603.20596](https://arxiv.org/abs/2603.20596).
- [22] B. Singh, B.K. Singh and D.V. Singh, *Thermodynamics, phase structure of Bardeen massive black hole in Gauss-Bonnet gravity*, *Int. J. Geom. Meth. Mod. Phys.* **20** (2023) 2350125.

- [23] H. Zeng and Y. Meng, *Images from disk and spherical accretions of Bardeen black hole surrounded by perfect fluid dark matter*, *Phys. Lett. B* **876** (2026) 140434 [2512.05147].
- [24] V. Vertogradov and A. Rincon, *Energy extraction and evolution of regular black holes: The case of Bardeen spacetime*, *Phys. Dark Univ.* **50** (2025) 102066 [2508.14489].
- [25] R.A. Konoplya and A. Zhidenko, *Dymnikova black hole from an infinite tower of higher-curvature corrections*, *Phys. Lett. B* **856** (2024) 138945 [2404.09063].
- [26] M. Alshammari, S. Alshammari, S. Khan and M.M. Al-sawalha, *Einasto-core generalization of the Dymnikova regular black hole metric*, *Eur. Phys. J. C* **85** (2025) 1402.
- [27] V. Vertogradov, *Gravitational collapse and formation of regular black holes: Dymnikova, Hayward, and beyond*, *Eur. Phys. J. C* **85** (2025) 839 [2504.19292].
- [28] M. Fathi, M. Molina and J.R. Villanueva, *Adiabatic evolution of Hayward black hole*, *Phys. Lett. B* **820** (2021) 136548 [2101.12253].
- [29] M.M. Gohain, K. Bhuyan, R. Borgohain, T. Gogoi, K. Bhuyan and P. Phukon, *Frolov black hole surrounded by quintessence - I: Thermodynamics, geodesics and shadows*, *Nucl. Phys. B* **1018** (2025) 117073 [2412.06252].
- [30] S. Bora, D.J. Gogoi and P.K. Karmakar, *Impact of Thermodynamic Corrections on the Stability of Hayward-Anti de Sitter Black Hole Surrounded by a Fluid of Strings*, 2510.04208.
- [31] A. Waseem, F. Javed, G. Mustafa, S.K. Maurya, F. Atamurotov and M. Shrahili, *Joule–Thomson expansion of Hayward-AdS black hole surrounded by fluid of strings*, *Annals Phys.* **480** (2025) 170087.
- [32] Q.-Q. Liang, Z. Cai, D. Liu and Z.-W. Long, *Observational properties and quasinormal Modes of the Hayward black Hole surrounded by a cloud of strings*, 2511.02396.
- [33] T. Naseer, J. Levi Said, R. Altuijri, M.R. Eid and A.-H. Abdel-Aty, *Spherically symmetric regular Hayward black hole and its thermodynamic properties: Insights via gravitational decoupling*, *Int. J. Geom. Meth. Mod. Phys.* **22** (2025) 2540055.
- [34] E. Ayon-Beato and A. Garcia, *New regular black hole solution from nonlinear electrodynamics*, *Phys. Lett. B* **464** (1999) 25 [hep-th/9911174].
- [35] E. Ayon-Beato and A. Garcia, *The Bardeen model as a nonlinear magnetic monopole*, *Phys. Lett. B* **493** (2000) 149 [gr-qc/0009077].
- [36] I. Dymnikova, *Regular electrically charged structures in nonlinear electrodynamics coupled to general relativity*, *Class. Quant. Grav.* **21** (2004) 4417 [gr-qc/0407072].
- [37] L. Balart and E.C. Vagenas, *Regular black holes with a nonlinear electrodynamics source*, *Phys. Rev. D* **90** (2014) 124045 [1408.0306].
- [38] H. Culetu, *On a regular charged black hole with a nonlinear electric source*, *Int. J. Theor. Phys.* **54** (2015) 2855 [1408.3334].
- [39] Z.-Y. Fan and X. Wang, *Construction of Regular Black Holes in General Relativity*, *Phys. Rev. D* **94** (2016) 124027 [1610.02636].
- [40] D.V. Singh, S.G. Ghosh and S.D. Maharaj, *Exact nonsingular black holes and thermodynamics*, *Nucl. Phys. B* **981** (2022) 115854.
- [41] K.A. Bronnikov, *Regular black holes sourced by nonlinear electrodynamics*, 2211.00743.
- [42] A.A. Araújo Filho, E.L.B. Junior, J.T.S.S. Junior, F.S.N. Lobo, J.A.A. Ramos, M.E. Rodrigues et al., *Regular Black Holes in General Relativity from Nonlinear Electrodynamics with de Sitter Cores*, 2604.20066.
- [43] C. Liu, T. Zhu, Q. Wu, K. Jusufi, M. Jamil, M. Azreg-Aïnou et al., *Shadow and quasinormal modes of a rotating loop quantum black hole*, *Phys. Rev. D* **101** (2020) 084001 [2003.00477].

- [44] M. Cadoni, M. Oi and A.P. Sanna, *Effective models of nonsingular quantum black holes*, *Phys. Rev. D* **106** (2022) 024030 [2204.09444].
- [45] G.S. M and S. Das, *EHT-Constrained Analysis of Shadow Deformation in Quantum-Improved Rotating Non-Singular Magnetic Monopole*, [2604.04695](#).
- [46] J. Borissova and R. Carballo-Rubio, *Effective geometrodynamics for renormalization-group improved black-hole spacetimes in spherical symmetry*, [2601.17115](#).
- [47] V. Vertogradov and A. Övgün, *Exact regular black hole solutions with de Sitter cores and Hagedorn fluid*, *Class. Quant. Grav.* **42** (2025) 025024 [2408.02699].
- [48] N. Heidari, A.A. Araújo Filho, V. Vertogradov and A. Övgün, *Black hole with a de Sitter core: classical and quantum features*, [2412.05072](#).
- [49] A. Simpson and M. Visser, *Regular black holes with asymptotically Minkowski cores*, *Universe* **6** (2019) 8 [1911.01020].
- [50] A. Simpson and M. Visser, *The eye of the storm: a regular Kerr black hole*, *JCAP* **03** (2022) 011 [2111.12329].
- [51] A. Simpson and M. Visser, *Black-bounce to traversable wormhole*, *JCAP* **02** (2019) 042 [1812.07114].
- [52] F.S.N. Lobo, M.E. Rodrigues, M.V. de Sousa Silva, A. Simpson and M. Visser, *Novel black-bounce spacetimes: wormholes, regularity, energy conditions, and causal structure*, *Phys. Rev. D* **103** (2021) 084052 [2009.12057].
- [53] A. Ditta, T. Xia, R. Ali, G. Mustafa, G. Mustafa and A. Mahmood, *Thermal properties of simpson-visser minkowski core regular black holes solution in verlinde’s emergent gravity*, *Physics of the Dark Universe* **43** (2024) 101418.
- [54] H.-W. Hu, C. Lan and Y.-G. Miao, *A regular black hole as the final state of evolution of a singular black hole*, *Eur. Phys. J. C* **83** (2023) 1047 [2303.03931].
- [55] M. Estrada and R. Aros, *Pure Lovelock gravity regular black holes*, *JCAP* **01** (2025) 032 [2409.09559].
- [56] P. Bueno, P.A. Cano and R.A. Hennigar, *Regular black holes from pure gravity*, *Phys. Lett. B* **861** (2025) 139260 [2403.04827].
- [57] S. Capozziello, S. De Bianchi and E. Battista, *Avoiding singularities in Lorentzian-Euclidean black holes: The role of atemporality*, *Phys. Rev. D* **109** (2024) 104060 [2404.17267].
- [58] F. Zhang, *Black holes as portals to an Euclidean realm*, [2603.25313](#).
- [59] J. Borissova, S. Liberati and M. Visser, *Timelike convergence condition in regular black-hole spacetimes with (anti-)de Sitter core*, *Phys. Rev. D* **112** (2025) 104072 [2509.08590].
- [60] T. Jacobson, *When is  $g(tt)g(rr) = -1$ ?*, *Class. Quant. Grav.* **24** (2007) 5717 [0707.3222].
- [61] J. Ovalle, *Black holes without Cauchy horizons and integrable singularities*, *Phys. Rev. D* **107** (2023) 104005 [2305.00030].
- [62] R. Casadio, A. Kamenshchik and J. Ovalle, *From black hole mimickers to black holes*, *Phys. Rev. D* **109** (2024) 024042 [2401.03980].
- [63] R.P. Geroch, *What is a singularity in general relativity?*, *Annals Phys.* **48** (1968) 526.
- [64] G.J. Olmo, D. Rubiera-Garcia and A. Sanchez-Puente, *Geodesic completeness in a wormhole spacetime with horizons*, *Phys. Rev. D* **92** (2015) 044047 [1508.03272].
- [65] C.B. Owen, N. Yunes and H. Witek, *Petrov type, principal null directions, and Killing tensors of slowly rotating black holes in quadratic gravity*, *Phys. Rev. D* **103** (2021) 124057 [2103.15891].

- [66] C. Cherubini, D. Bini, S. Capozziello and R. Ruffini, *Second order scalar invariants of the Riemann tensor: Applications to black hole space-times*, *Int. J. Mod. Phys. D* **11** (2002) 827 [[gr-qc/0302095](#)].
- [67] Y.N. Obukhov and F.W. Hehl, *On the relation between quadratic and linear curvature Lagrangians in Poincare gauge gravity*, *Acta Phys. Polon. B* **27** (1996) 2685 [[gr-qc/9602014](#)].
- [68] A. Steane, *Relativity Made Relatively Easy Volume 2: General Relativity and Cosmology*, Oxford University Press, Oxford (2021).
- [69] R. Jackiw and S.Y. Pi, *Chern-Simons modification of general relativity*, *Phys. Rev. D* **68** (2003) 104012 [[gr-qc/0308071](#)].
- [70] J. Carminati and R.G. McLenaghan, *Algebraic invariants of the Riemann tensor in a four-dimensional Lorentzian space*, *J. Math. Phys.* **32** (1991) 3135.
- [71] E. Zakhary and C.B.G. McIntosh, *A Complete Set of Riemann Invariants*, *Gen. Rel. Grav.* **29** (1997) 539.
- [72] J. Borissova and R. Carballo-Rubio, *Regular black holes from pure gravity in four dimensions*, [2602.16773](#).
- [73] C.W. Misner, K.S. Thorne and J.A. Wheeler, *Gravitation*, W. H. Freeman, San Francisco (1973).
- [74] M. Nakahara, *Geometry, topology and physics* (2003).
- [75] E. Poisson, *A Relativist's Toolkit: The Mathematics of Black-Hole Mechanics*, Cambridge University Press (12, 2009), [10.1017/CBO9780511606601](#).
- [76] L. Rezzolla and O. Zanotti, *Relativistic Hydrodynamics*, Oxford University Press (9, 2013), [10.1093/acprof:oso/9780198528906.001.0001](#).
- [77] H. Maeda, *Hawking-Ellis type of matter on Killing horizons in symmetric spacetimes*, *Phys. Rev. D* **104** (2021) 084088 [[2107.01455](#)].
- [78] F.R. Klinkhamer, *A new type of nonsingular black-hole solution in general relativity*, *Mod. Phys. Lett. A* **29** (2014) 1430018 [[1309.7011](#)].
- [79] F.R. Klinkhamer, *On a soliton-type spacetime defect*, *J. Phys. Conf. Ser.* **1275** (2019) 012012 [[1811.01078](#)].
- [80] F.R. Klinkhamer and Z.L. Wang, *Nonsingular bouncing cosmology from general relativity*, *Phys. Rev. D* **100** (2019) 083534 [[1904.09961](#)].
- [81] E. Battista, *Nonsingular bouncing cosmology in general relativity: physical analysis of the spacetime defect*, *Class. Quant. Grav.* **38** (2021) 195007 [[2011.09818](#)].
- [82] V. Faraoni, A. Giusti and T.F. Bean, *Asymptotic flatness and Hawking quasilocal mass*, *Phys. Rev. D* **103** (2021) 044026 [[2010.00069](#)].
- [83] Z.-L. Wang and E. Battista, *Energy conditions in static, spherically symmetric spacetimes and effective geometries*, [2604.16545](#).
- [84] X. Liang, Y.-P. Hu, C.-H. Wu and Y.-S. An, *Thermodynamics and evaporation of perfect fluid dark matter black hole in phantom background*, *Eur. Phys. J. C* **83** (2023) 1009 [[2308.00308](#)].
- [85] M. Abramowitz, I.A. Stegun et al., *Handbook of mathematical functions*, vol. 10, Dover, New York (1968).
- [86] K.A. Bronnikov and J.C. Fabris, *Regular phantom black holes*, *Phys. Rev. Lett.* **96** (2006) 251101 [[gr-qc/0511109](#)].
- [87] A. Kar and S. Kar, *Diverse regular spacetimes using a parametrised density profile*, *Eur. Phys. J. C* **85** (2025) 773 [[2504.12042](#)].

- [88] J.C.S. Neves and A. Saa, *Regular rotating black holes and the weak energy condition*, *Phys. Lett. B* **734** (2014) 44 [[1402.2694](#)].
- [89] R.A. Konoplya and A. Zhidenko, *Dark matter halo as a source of regular black-hole geometries*, *Phys. Rev. D* **113** (2026) 043011 [[2511.03066](#)].
- [90] S. Bahamonde, *Geometrically Regular Black Holes with Hedgehog Scalar Hair*, [2604.15758](#).
- [91] J. Einasto, *Dark Matter*, 1, 2009 [[0901.0632](#)].
- [92] Retana-Montenegro, E. and Van Hese, E. and Gentile, G. and Baes, M. and Frutos-Alfaro, F., *Analytical properties of Einasto dark matter haloes*, *Astronomy and Astrophysics* **540** (2012) .
- [93] L. Xiang, Y. Ling and Y.G. Shen, *Singularities and the Finale of Black Hole Evaporation*, *Int. J. Mod. Phys. D* **22** (2013) 1342016 [[1305.3851](#)].
- [94] W. Dehnen, *A Family of Potential-Density Pairs for Spherical Galaxies and Bulges*, *Mon. Not. Roy. Astron. Soc.* **265** (1993) 250.
- [95] J.F. Navarro, C.S. Frenk and S.D.M. White, *The Structure of cold dark matter halos*, *Astrophys. J.* **462** (1996) 563 [[astro-ph/9508025](#)].
- [96] L. Hernquist, *An Analytical Model for Spherical Galaxies and Bulges*, *Astrophys. J.* **356** (1990) 359.
- [97] H. Zhao, *Analytical models for galactic nuclei*, *Mon. Not. Roy. Astron. Soc.* **278** (1996) 488 [[astro-ph/9509122](#)].
- [98] EVENT HORIZON TELESCOPE collaboration, *First M87 Event Horizon Telescope Results. I. The Shadow of the Supermassive Black Hole*, *Astrophys. J. Lett.* **875** (2019) L1 [[1906.11238](#)].
- [99] EVENT HORIZON TELESCOPE collaboration, *First Sagittarius A\* Event Horizon Telescope Results. I. The Shadow of the Supermassive Black Hole in the Center of the Milky Way*, *Astrophys. J. Lett.* **930** (2022) L12 [[2311.08680](#)].
- [100] V. Cardoso and P. Pani, *Testing the nature of dark compact objects: a status report*, *Living Rev. Rel.* **22** (2019) 4 [[1904.05363](#)].
- [101] S. Vagnozzi et al., *Horizon-scale tests of gravity theories and fundamental physics from the Event Horizon Telescope image of Sagittarius A*, *Class. Quant. Grav.* **40** (2023) 165007 [[2205.07787](#)].
- [102] V. Vertogradov and A. Övgün, *General approach on shadow radius and photon spheres in asymptotically flat spacetimes and the impact of mass-dependent variations*, *Phys. Lett. B* **854** (2024) 138758 [[2404.18536](#)].
- [103] Z.-L. Wang and E. Battista, *Dynamical features and shadows of quantum Schwarzschild black hole in effective field theories of gravity*, *Eur. Phys. J. C* **85** (2025) 304 [[2501.14516](#)].
- [104] Z.-L. Wang, *Exploring the role of accretion disk geometry in shaping black hole shadows*, *Phys. Rev. D* **112** (2025) 064052 [[2506.21148](#)].
- [105] W. Liu, Y. Liu, D. Wu and Y.-X. Liu, *A Universal Framework for Horizon-Scale Tests of Gravity with Black Hole Shadows*, [2511.06017](#).
- [106] Q. Sun, Y. Zhang, C.-H. Xie and Q.-Q. Li, *Shadow of Kerr black hole surrounded by a cloud of strings in Rastall gravity and constraints from M87\**, *Phys. Dark Univ.* **46** (2024) 101599 [[2401.08693](#)].
- [107] S.-W. Wei and Y.-X. Liu, *Gravity/thermodynamics correspondence via black hole shadows*, [2604.04441](#).
- [108] I. Dymnikova, *Spherically symmetric space-time with the regular de Sitter center*, *Int. J. Mod. Phys. D* **12** (2003) 1015 [[gr-qc/0304110](#)].

- [109] E. Poisson and W. Israel, *Inner-horizon instability and mass inflation in black holes*, *Phys. Rev. Lett.* **63** (1989) 1663.
- [110] A. Ori, *Inner structure of a charged black hole: An exact mass-inflation solution*, *Phys. Rev. Lett.* **67** (1991) 789.
- [111] R. Carballo-Rubio, F. Di Filippo, S. Liberati, C. Pacilio and M. Visser, *On the viability of regular black holes*, *JHEP* **07** (2018) 023 [[1805.02675](#)].
- [112] S. Rosswog, *SPH Methods in the Modelling of Compact Objects*, *Liv. Rev. Comput. Astrophys.* **1** (2015) 1 [[1406.4224](#)].
- [113] C. Bambi et al., *Black hole mimickers: from theory to observation*, 5, 2025 [[2505.09014](#)].
- [114] V. De La Cruz and W. Israel, *Spinning shell as a source of the kerr metric*, *Phys. Rev.* **170** (1968) 1187.
- [115] L.S. Kegeles, *Collapse to a rotating black hole*, *Phys. Rev. D* **18** (1978) 1020.
- [116] W.-L. Qian, S. Chen, C.-G. Shao, B. Wang and R.-H. Yue, *Cuspy and fractured black hole shadows in a toy model with axisymmetry*, *Eur. Phys. J. C* **82** (2022) 91 [[2102.03820](#)].
- [117] L.-Y. Li, L.-M. Cao, Y. Gong, X.-Y. Liu and W. Zhou, *Signatures of the Israel Junction II: Double Photon Rings in Slowly Rotating Kerr Spacetime with Thin Shell*, [2602.07923](#).
- [118] M. Bouhmadi-López, C.-Y. Chen, X.Y. Chew, Y.C. Ong and D.-h. Yeom, *Traversable wormhole in Einstein 3-form theory with self-interacting potential*, *JCAP* **10** (2021) 059 [[2108.07302](#)].
- [119] E. Battista, S. Capozziello and A. Errehymy, *Generalized uncertainty principle corrections in Rastall–Rainbow Casimir wormholes*, *Eur. Phys. J. C* **84** (2024) 1314 [[2409.09750](#)].
- [120] M.R. Mehdizadeh and A.H. Ziaie, *Novel Casimir wormholes in Einstein gravity*, *Eur. Phys. J. Plus* **139** (2024) 1001 [[2406.03588](#)].
- [121] A. Xu, X.Y. Chew and D.-h. Yeom, *Dynamics of Bronnikov–Ellis wormhole with double-null simulation*, *JCAP* **08** (2025) 012 [[2503.07610](#)].
- [122] R.A. Konoplya and O.S. Stashko, *Transition from regular black holes to wormholes in covariant effective quantum gravity: Scattering, quasinormal modes, and Hawking radiation*, *Phys. Rev. D* **111** (2025) 084031 [[2502.05689](#)].
- [123] G. Li and Y.-Q. Wang, *Ellis–Bronnikov wormhole in Quasi-topological Gravity*, [2602.01029](#).
- [124] D. Jampolski and L. Rezzolla, *On the formation of gravastars*, [2509.15302](#).
- [125] H.-Y. Chen, Y. Hikida and Y. Koga, *AdS gravastar and its signatures from dual conformal field theory*, *Phys. Rev. Res.* **8** (2026) 023065 [[2512.01349](#)].
- [126] M.I.H. Sakib, W. Wang, X. Wu, M.G. Hafez and M.A. Kauser, *Relativistic formulation and physical viability of anisotropic analytic gravastars*, *Eur. Phys. J. C* **86** (2026) 310.
- [127] F. Rahaman, B.S. Choudhury, A. Sanyal, A. Islam and B. Samanta, *Exact gravastar solution*, *Phys. Lett. B* **876** (2026) 140412 [[2604.09719](#)].
- [128] H. Maeda, *Quest for realistic non-singular black-hole geometries: regular-center type*, *JHEP* **11** (2022) 108 [[2107.04791](#)].
- [129] S.M. Carroll, *Spacetime and Geometry: An Introduction to General Relativity*, Cambridge University Press (7, 2019), [10.1017/9781108770385](#).
- [130] A. Eichhorn and A. Held, *From a locality-principle for new physics to image features of regular spinning black holes with disks*, *JCAP* **05** (2021) 073 [[2103.13163](#)].
- [131] J. Overduin, M. Coplan, K. Wilcomb and R.C. Henry, *Curvature invariants for charged and rotating black holes*, *Universe* **6** (2020) .

- [132] G.V. Kraniotis, *Curvature Invariants for accelerating Kerr-Newman black holes in (anti-)de Sitter spacetime*, *Class. Quant. Grav.* **39** (2022) 145002 [[2112.01235](#)].
- [133] R. Maartens and B.A. Bassett, *Gravitoelectromagnetism*, *Class. Quant. Grav.* **15** (1998) 705 [[gr-qc/9704059](#)].
- [134] S. Weinberg, *Gravitation and Cosmology: Principles and Applications of the General Theory of Relativity*, John Wiley and Sons, New York (1972).
- [135] K.A. Bronnikov and S.G. Rubin, *Black Holes, Cosmology and Extra Dimensions*, WSP (2012), [10.1142/12186](#).
- [136] F.S.N. Lobo, M.E. Rodrigues, M.V. de Sousa Silva, A. Simpson and M. Visser, *Novel black-bounce spacetimes: wormholes, regularity, energy conditions, and causal structure*, *Phys. Rev. D* **103** (2021) 084052 [[2009.12057](#)].
- [137] I. Gkigkitzis, I. Haranas and O. Ragos, *Kretschmann Invariant and Relations Between Spacetime Singularities, Entropy and Information*, *Physics International* **5** (2014) 103 [[1406.1581](#)].